Journal of Environmental Chemical Engineering 14 (2026) 124229

Contents lists available at ScienceDirect

Journal of Environmental Chemical Engineering

journal homepage: www.elsevier.com/locate/jece

Production of secondary raw materials from the hydrotreating of plastic waste pyrolysis oils

Borja Baltasar Perez-Martinez [a,*], Petr Straka [b], Dan Vrtiška [b], Miloš Auersvald [b], Alexander Lopez-Urionabarrenechea [a]

[a] Chemical and Environmental Department, Faculty of Engineering of Bilbao, University of the Basque Country (UPV/EHU), Plaza Ingeniero Torres Quevedo, 1, Bilbao 48013, Spain

[b] Department of Sustainable Fuels and Green Chemistry, University of Chemistry and Technology Prague, Technická 5, 166 28 Prague 6, Czech Republic

ARTICLE INFO

Keywords:
Pyrolysis oil
Hydrotreating
Waste electrical and electronic equipment
Plastic waste
Chemical recycling

ABSTRACT

This study examines the upgrading of plastic waste pyrolysis oil (PWPO) derived from real waste electrical and electronic equipment (WEEE) and waste packaging (WP), with the objective of producing oil fractions for their valorization in material recycling strategies. The PWPO, rich in oxygen, nitrogen, sulfur, chlorine and bromine, was hydrotreated and subsequently fractionated into distillation cuts (naphtha, kerosene, atmospheric gas-oil and residue). The experiments were carried out in a continuous laboratory facility using two commercial hydrotreating catalysts: $NiMo/Al_2O_3$ and $CoMo/Al_2O_3$. These catalysts were tested in 5-day-long experiments, increasing the temperature by about 30 °C every 24 h, from 240 °C to 360 °C. In general, the NiMo catalyst performed better, yielding a hydrotreated oil virtually free of halogens at 360 °C. The naphtha fraction, representing almost half of the hydrotreated oil, contained neither sulfur nor nitrogen, and a proportion of benzene, toluene, ethylbenzene, and xylenes (BTEX) around 75 wt%, making it an alternative source of these valuable and widely used chemicals. In addition, naphthalene-rich kerosene and gas oil fractions were produced, with potential for use as a naphthalene oil source. The bottom residue fraction, yielding ≈ 20 wt%, could be reintroduced into refinery processes or used as marine fuel. These exceptional results enable the design of circular strategies for the production of petrochemicals from waste materials.

1. Introduction

Plastic waste pollution is one of the main environmental concerns of the 21st century. Plastics are versatile materials mainly used for packaging and construction, but they are also very common in automotive, electrical and electronic equipment (EEE), agriculture, gardening and farming, houseware, leisure and sports, and other sectors and products. Although the infrastructure to selectively sort plastic waste and the technology to recycle it do exist, in Europe, almost 25 wt% of the plastic waste that enters collection systems ends up in landfills [1]. There, plastic waste breaks down into micro- and nano-sized particles, causing a wide range of ecological problems and damage to human health [2,3].

Most of the plastic waste that ends up in landfills originates from the rejects produced by waste sorting plants, which concentrate all the materials that have not been selected or properly separated during the sorting process. These waste streams do not receive any further sorting or treatment due to economic or technical reasons and, given that, in most cases, are composed mainly of plastics, pyrolysis is a viable treatment alternative. This technique (heating in the absence of air) allows processing the waste without further separation, producing oils, gases, and char-like products from the thermal decomposition of the organic substances in the waste, including plastics [4]. The oil, commonly known as pyrolysis oil, has the potential to be processed in petroleum refining and/or petrochemical industries [5].

Abbreviations: AGO, atmospheric gas oil; BTEX, benzene, toluene, ethylbenzene and xylenes; BTX, benzene, toluene and xylenes; DMDS, dimethyl-disulfide; ED-XRF, energy dispersive X-ray fluorescence; EEE, electrical and electronic equipment; FCC, fluid catalytic cracking; HDN, hydrodenitrogenation; HDS, hydrodesulfurization; HDX, hydrodehalogenation; LCO, light cycle oil; PVC, polyvinyl chloride; PWPO, plastic waste pyrolysis oil; SAF, sustainable aviation fuel; SPK, synthetic paraffinic kerosene; SRGO, straight-run gas oil; WEEE, waste electrical and electronic equipment; WHSV, weight hourly space velocity; WP, waste packaging.

* Corresponding author.
E-mail address: borjabaltasar.perez@ehu.eus (B.B. Perez-Martinez).

https://doi.org/10.1016/j.jece.2026.124229
Received 25 May 2026; Received in revised form 9 July 2026; Accepted 19 July 2026
Available online 21 July 2026
2213-3437/© 2026 The Authors. Published by Elsevier Ltd. This is an open access article under the CC BY license (http://creativecommons.org/licenses/by/4.0/).

The main oil and petrochemical companies in Europe are today involved in testing programs for plastic waste pyrolysis oils (PWPO) at industrial scale. The idea behind this practice is clear: PWPO can be a source of raw materials for producing new plastics, helping to achieve the recycled content already established by European legislation for packaging plastics and, soon, also for automotive plastics [6]. However, PWPO cannot be directly used for monomer or base chemicals production through traditional routes, due to its broad boiling point distribution, complex composition, high olefin content, heteroatoms contamination (S, N, O, halogens, etc.) and chemical instability [7–9]. Besides, the quality of the PWPO strongly depends on the composition of the plastics and other materials in the waste stream. In this sense, PWPO originating from waste EEE (WEEE) plastics or technical plastic waste is typically more contaminated with heteroatoms and exhibits a higher degree of aromaticity than those produced from packaging plastic waste [10].

In this sense, the main issue concerning this kind of oil is the high concentration of chlorine (0.5–10 wt%), bromine (0.1–2.2 wt%) and styrene (> 12 wt%) [11–13]. The formers must be eliminated almost entirely in order to be processed in the petroleum-based industry, as they are elements that are completely foreign to the usual chemistry of fossil crude oil, which is reported to have a maximum 7 mg kg^{-1} of chlorine (mainly inorganic chlorine contrary to organic chlorine in PWPO) and no bromine [14]. On the other hand, styrene is an instable chemical with tendency to polymerize, which can generate processing and storage issues derived from gum formation [15].

Hydroprocessing, particularly hydrotreating, is the most studied upgrading process for PWPO [16–19]. This technique is typically conducted at temperatures between 250 °C and 400 °C in the presence of hydrogen and solid catalysts and it is a well-established process in the oil industry, typically applied to remove sulfur, nitrogen, oxygen, metals, aromatics and olefins from petroleum fractions [20–22]. It has been also intensively studied to upgrade the liquid fraction of biomass pyrolysis, mainly with the aim of removing oxygen [23–24]. Related to PWPO, hydrotreating has been reported to be effective in the removal of nitrogen, sulfur and olefins in order to obtain PWPO fractions that meet the specifications of fuels such as kerosene or diesel [25–28]. Recently, the production of naphtha via hydrotreating of PWPO for steam cracking has also been explored [29]. However, the PWPO used in the vast majority of studies on hydrotreating comes from waste packaging plastics and tires, where halogen concentrations are usually low [30–31]. The hydrodechlorination of highly chlorinated PWPO has been scarcely studied and usually in presence of expensive catalysts such as platinum based catalysts [32]. However, it is necessary to study the performance of traditional hydrotreatment catalysts (NiMo and CoMo on alumina) in the processing of highly chlorinated PWPO, bearing in mind that PWPO is a waste-derived product and the economic viability of the process is always a factor to consider. Besides, no information on hydrotreatment's capacity to remove bromine has been found in the literature, so these traditional hydrotreatment catalysts will be proved for the first time in presence of bromine. At last, there is a lack of research assessing the potential of hydrotreated PWPO fractions as feedstock for recycling processes beyond fuel utilization.

This paper presents the upgrading of halogenated pyrolysis oils derived from WEEE plastics and waste packaging (WP) plastics through a combined hydrotreatment and distillation process. The hydrotreatment of such a halogenated mixture of pyrolysis oils is innovative in the field, as is the search for applications that substitute raw materials with hydrotreated and distilled PWPO products. The motivation behind this work is to expand the sources of pyrolysis oils for petrochemical processes, enabling particularly contaminated and unstable oils to be part of circular plastic production routes.

2. Materials and methods

2.1. Materials

15 L of plastic waste pyrolysis oil (PWPO) were prepared by mixing 8 L of WP pyrolysis oil, 5 L of WEEE pyrolysis oil and 2 L of styrene. WP and WEEE pyrolysis oils were real pyrolysis liquids provided by Nantek (Spain), a technology and energy company that has developed its own technology to convert non-recyclable plastic waste into renewable energy and advanced second-life fuels, positioning it as a leader in the transition to a circular economy and decarbonization. WP pyrolysis oil was produced in a 1500 L semi-industrial scale batch reactor, while WEEE pyrolysis oil was produced in a 40 L tank reactor operating in a semi-batch regime. More details cannot be addressed due to confidentiality issues. Styrene (≥ 99%, stabilized with 4-tert-butylcatechol) was purchased from Sigma-Aldrich. WP pyrolysis oil was added to WEEE pyrolysis oil in order to prevent catalyst poisoning by not exceeding the chlorine content of 1000 mg kg^{-1} and the total halogens content of 1200 mg kg^{-1}. This addition diluted the styrene concentration of WEEE oil, so, commercial grade styrene was mixed with the blend of both oils to reach a styrene concentration around 15 wt%, typical of pyrolysis oils from WEEE plastics [11,12]. As can be seen in Figure S1, PWPO was a low viscosity dark brown liquid (color 7.5–8.0 according to ASTM D1500–12 standard). Two commercial hydrotreating catalysts were used in this study: NiMo/γ-Al_2O_3 and CoMo/γ-Al_2O_3. Their basic properties are summarized in Table S1.

2.2. Hydrotreatment experiments

The hydrotreatment experiments were performed in a lab-scale fixed-bed hydrotreating unit (CACTU Solutions, Czech Republic) with a co-current flow of liquid and hydrogen. The hydrotreating unit is equipped with a high-pressure feeding pump, a hydrogen mass-flow controller, a tubular reactor with an internal diameter of 23 mm and a length of 490 mm (placed in a four-zone furnace), and a high-pressure gas-liquid separator (see Fig. 1). For more details, see a previous work from the authors [33]. The reaction temperature in the catalyst bed was controlled by six thermocouples placed along the reactor axis, and the experimental temperature was calculated as the arithmetic average of the thermocouple readings.

Glass beads (2 mm in diameter) were placed in the upper preheating zone of the reactor. Then, the reactor was filled with a mixture of catalyst (250–590 μm particle size) and silicon carbide (SiC) in a volumetric ratio of 1:2 (catalyst:SiC). This catalyst bed was placed in the center part of the reactor. SiC was used with the aim of improving fluid dynamics and heat transfer in the fixed bed, and it was considered chemically inert in the process conditions. On the one hand, the dilution of catalyst particles with hard SiC particles avoids preferential routes that may arise due to sintering of catalyst particles. On the other hand, the good thermal conductivity and stability of SiC help obtaining quasi-isothermal operation due to its ability to decrease the heat release per unit volume and to avoid hot spots, by enhancing heat conduction in the bed [34].

Concerning catalytic bed porosity (ε), it was calculated to be 0.38, by using the empirical correlation proposed by Pushnov for particles of irregular shapes [35]. For this calculation, a mean catalyst particle size of 420 mm (d) and the reactor diameter of 23 mm (D) were used, giving a diameters ratio (D/d) of 54.8. Other porosity correlations for packed bed reactors reported by Guo et al. were also checked, verifying that porosity values were in the range 0.36–0.40 [36]. So, the estimation of $\varepsilon = 0.38$ was considered valid. Porosity is a key issue in fixed bed reactors, since it influences fluid dynamics, pressure drop, and mass and heat transfer. In general terms, the higher the porosity, the lower the pressure drop and the pore velocity, which can hinder the mass and heat transfer, since conduction and convection decrease. However, although low porosities enhance mass and heat transfer, pressure drop can become a big

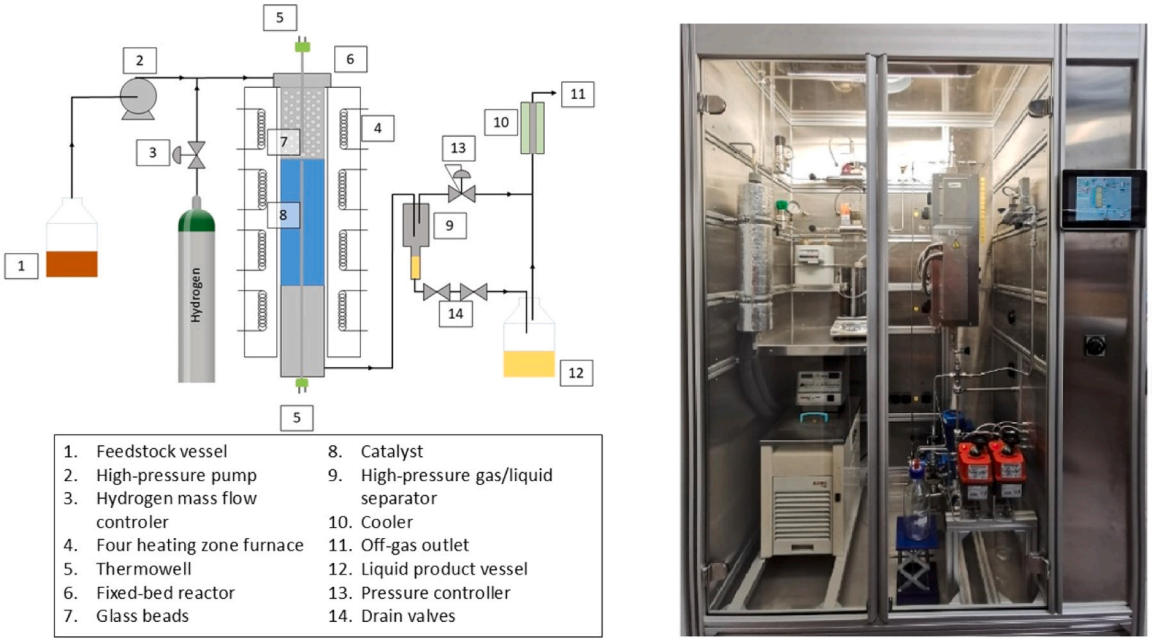


Fig. 1. Schematic drawing (left) and a picture (right) of the laboratory scale hydrotreatment plant (CACTU Solutions, Czech Republic).

operational issue at very low porosity values. The porosity used in this study lied in the range 0.36–0.42, typically used for randomly fixed beds, and close to the theoretical lower limit of 0.36, with the aim of maximizing mass and heat transfer while maintaining assumable pressure drop [37,38].

Before the experiments, the catalysts were dried, sulfidized and stabilized in situ. Drying was carried out at 120 °C and 0.5 MPa for 3 h, in the presence of 30 L h^{-1} of hydrogen. Activation was performed using straight-run gas oil (SRGO) containing 1.28 wt% of sulfur, mixed with 3.0 wt% of dimethyl-disulfide (DMDS). The activation program consisted of heating from 150 to 345 °C at 20 °C h^{-1} and maintaining at 345 °C for 6 h, with a weight hourly space velocity (WHSV) of 1 h^{-1}, a pressure of 4 MPa and a hydrogen-to-feedstock ratio of 230 m^3 m^{-3}. After activation, the catalyst activity was stabilized with SRGO at 290 °C and 4 MPa, WHSV of 1 h^{-1}, and a hydrogen to feedstock ratio of 230 m^3 m^{-3} for 48 h.

Two week-long experiments were carried out in this study, consisting of testing each catalyst continuously for 5 days (120 h of time-on-stream corresponding to the feeding of PWPO) with an increase of reaction temperature every 24 h (240–270–300–330–360°C). Table S2 shows the temperatures used in the experiments and the designation employed. The objective of this experimental procedure was to study the influence of temperature in the hydrotreating process, although catalyst deactivation with time may be also taken into account. In this sense, feedstock was spiked with 0.15 wt% of DMDS in order to maintain the catalyst activity during the experimental run.

In both experiments, hydrotreated liquid products (called primary liquids) and generated gases were sampled at each temperature for characterization. Apart from temperature, the experiments were carried out at the following fixed operational conditions: PWPO flow rate of 32 g h^{-1}, hydrogen flow rate of 14 L h^{-1}, 32 g of catalyst and total pressure of 10 MPa. This means a WHSV of 1 h^{-1} and a hydrogen to feedstock ratio of 400 m^3 m^{-3}. It must be said that the highest temperature (360 °C) could not be tested with the CoMo catalyst due to increased pressure drop in the reactor at the end of the test. This was primarily due to the deposition of solids (mostly NH_4Cl) at the reactor outlet. This issue, which was currently limited to a laboratory-scale experimental problem, must be taken into account when scaling up this process to larger scales and continuous operation, as it could become a limiting factor in the process. In this regard, future research should focus on characterizing the fixed bed to determine whether the pressure drop is indeed caused by NH_4Cl deposition and, if so, propose solutions.

2.3. Analytical techniques

Total carbon, hydrogen and nitrogen were determined in a LECO CHN TrueSpec automatic analyzer (LECO, USA) following the procedure described in the EN ISO 21663:2021 standard, while total sulfur and nitrogen in the products were quantified on a trace elemental analyzer TS−100 (Mitsubishi, Japan), according to the ASTM D5453 and ASTM D4629 procedures, respectively. Chlorine and bromine were determined by ICP-OES Optima 8000 (Perkin-Elmer, USA) after microwave-induced combustion of the sample. Elemental analysis was completed with the analysis of the metal content of the PWPO via energy dispersive X-ray fluorescence (ED-XRF) on a Rigaku NEX DE ED-XRF spectrometer (Rigaku, USA) by means of standard-less semi-quantitative analysis method.

PWPO and primary hydrotreated liquids were fractionated into naphtha (< 150 °C), kerosene (150–250 °C), atmospheric gas oil (AGO) (250–360 °C) and bottom residue (> 360 °C) using an automatic distillation apparatus (Fischer Technology, USA) equipped with a Spaltrohr column [33]. Each of these fractions was then separately characterized. The density and kinematic viscosity of liquid products were measured by SVM 3000 Stabinger Viscometer (Anton Paar, Austria), following the ASTM D4052 and D445 methods, respectively. Before the characterization of primary hydrotreated liquids, they were subjected to wet cleaning with sodium hydroxide and boric acid in order to desorb the absorbed acid and basic gases, respectively.

Compositional analysis of liquid samples was carried out using an Agilent 8890 GC × GC-FID/MS (Agilent Technologies, USA) equipped with a reverse fill-flush flow modulator (SepSolve Analytical, UK) and a reverse configuration of columns [39]. Group type composition was carried out following the ASTM D8396 method, while the olefin content was determined by a method based on their selective adsorption over $AgNO_3/SiO_2$. For more details about the methodology applied, the readers are kindly referred to the respective reference [40]. The saturated hydrocarbons of the residue fraction were separated and

quantified using a preparative liquid column chromatography method extensively described in previous work [41]. The gaseous products were analyzed via Agilent 6890 N gas chromatograph with a flame ionization detector equipped with an Agilent J&W CP CARBOBOND capillary column (50 m × 0.53 mm × 50 μm) (Agilent Technologies, USA).

3. Results

3.1. Characterization of PWPO

The density and elemental analysis of PWPO are shown in Table 1. Density was found to be 911 kg m^{-3}, a value similar to the density of marine fuels [42], and higher than the typical densities of WP plastics pyrolysis oil, which are reported to be in the range 760–850 kg m^{-3} [9, 43]. The density of PWPO was also higher than that of tire pyrolysis oils, which is typically lower than 900 kg m^{-3} [33,42]. The high density of PWPO was related to its high aromatics and hetero-compounds content. Concerning the elemental composition, it was dominated by carbon (86.5 wt%) and hydrogen (9.6 wt%), followed by oxygen (2.7 wt%). Carbon content was higher than the typical values for WEEE plastics pyrolysis oil, which are normally in the range 70–80 wt% [44,45], and similar to that of WP plastics pyrolysis oils (> 80 wt%) [8]. This was due to the fact that the proportion of WEEE plastic pyrolysis oil in the used mixture was 33 vol%, with the rest consisting of WP plastics pyrolysis oil and styrene. The main detected non-metallic pollutants of PWPO were the already mentioned oxygen (2.7 wt%), nitrogen (7000 mg kg^{-1}), sulfur (337 mg kg^{-1}), chlorine (837 mg kg^{-1}) and bromine (346 mg kg^{-1}). These pollutants were at lower concentrations than in pyrolysis oils from WEEE plastics [13], again due to the dilution by the pyrolysis oil from WP and styrene to meet the total halogen limit for the used catalysts. Concerning metal content, silicon (1770 mg kg^{-1}), magnesium (1159 mg kg^{-1}) and aluminum (733 mg kg^{-1}) were found in the highest concentrations, together with smaller quantities of phosphorus, iron, nickel and zinc. The origin of silicon could be related to the presence of polysiloxanes (silicones) as electric insulators, protective coatings or part of cables of EEE [46], while magnesium is present in several flame retardant systems used for epoxy resins and PVC, also common materials in EEE [47,48]. In fact, the flame retardant system of epoxy resins can be comprised both magnesium and silicon [49].

Fig. 2 shows the distillation yields of the PWPO. Naphtha cut was the main fraction of PWPO, yielding almost 50 wt%. The naphtha yield was higher than reported for other types of plastic-derived pyrolysis oils. Zeb et al. obtained lower yields for the light fractions of packaging-derived pyrolysis oils, specifically 30 wt% and 22.4 wt% for distillates at temperatures up to 175 °C [14]. Arjharn et al. also obtained 30 wt% of distillate at temperatures below 175 °C working with WP plastic pyrolysis oil [50]. On the other hand, Straka et al. reported around 30 wt%

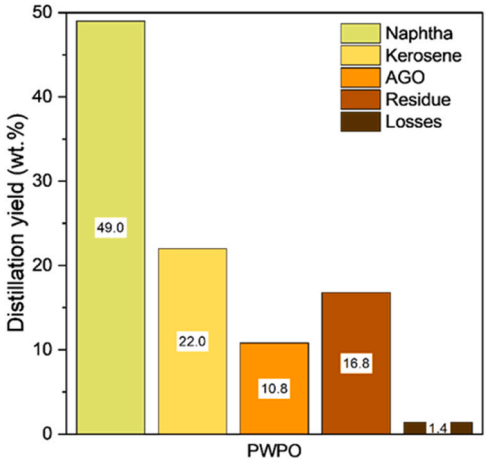


Fig. 2. PWPO distillation yields.

of naphtha working with tire pyrolysis oils [33]. Therefore, this was a very interesting result since naphtha is normally the most desirable distillation fraction for the production of base chemicals in the petrochemical industry [51]. The second fraction in weight was kerosene (22.0 wt%), followed by residue (16.8 wt%), which showed a higher yield than atmospheric gas oil (10.8 wt%). The high percentage of bottom residue (> 360 °C) is explained by the fact that plastic pyrolysis oils typically exhibit final boiling points higher than 500 °C [52].

Table 2 shows the composition of the distillation cuts of PWPO. Overall, the composition showed that aromatic hydrocarbons were dominant in the studied PWPO. This was directly related to the composition of the pyrolysis oils blended to make the PWPO (oils from real plastic rejects of WP and WEEE), as well as to pure styrene. On the one hand, the plastic rejects from WP are typically a mixture of packaging and non-packaging plastics, along with other non-plastic materials, which typically produce higher yields of aromatics than pure polyolefins [7]. On the other hand, WEEE plastics are known to produce aromatic hydrocarbons in high quantities under pyrolysis conditions [11–12]. Regarding the non-hydrocarbons, phenolic chemicals and nitriles, such as benzenebutanenitrile, were qualitatively detected (not reported in Table 2). It must be said that non-hydrocarbons compounds in GCxGC mean compounds eluting out of the hydrocarbon region, i.e., very polar compounds containing heteroatoms. However, aliphatic hetero-compounds elute in the naphthenes/aromatic region, therefore, "non-hydrocarbons" refer to a subgroup of total hetero-compounds.

Aromatic hydrocarbons in the range C_6-C_{10} (benzene + alkyl-

Table 1
Density and elemental analysis of PWPO.

Parameter	Units	
Density at 15 °C	kg m^{-3}	911
C	wt%	86.5
H		9.6
N		0.7
O		2.7
S	mg kg^{-1}	337
Cl		837
Br		346
Si	mg kg^{-1}	1770
Mg		1159
Al		733
P		200
Fe		58
Ni		11
Zn		6

Table 2
Composition of PWPO derived distillation fractions (wt%).

		Naphtha	Kerosene	AGO
Non-hydrocarbons		4.1	21.4	13.4
Saturated hydrocarbons		7.8	5.7	8.3
Olefins		8.4	16.6	19.5
Total Aromatics		79.7	56.3	58.8
Benzene		11.5	< 0.01	-[1]
Alkyl-benzenes	Toluene	16.8	0.02	-[1]
	o-Xylene	0.9	0.2	-[1]
	m/p-Xylene	3.0	-[1]	-[1]
	Ethylbenzene	11.5	0.9	-[1]
	Styrene	33.2	11.4	1.1
	Others	2.8	12.5	1.6
Total Alkylbenzenes		68.2	25.0	2.7
Cyclo-aromatics		-[1]	12.8	2.1
Di-aromatics	Naphthalenes	-[1]	18.4	15.3
	Biphenyls	-[1]	0.1	22.8
Tri-aromatics		-[1]	-[1]	14.6
Tetra-aromatics		-[1]	-[1]	1.4

[1] Not detected.

benzenes) were by far the main components of naphtha cut (79.7 wt%), highlighting styrene, with a concentration of 33.2 wt%. Apart from aromatic hydrocarbons, lower quantities of saturated hydrocarbons (7.8 wt%) and olefins (8.4 wt%) were also measured, followed by non-hydrocarbons (4.1 wt%), where heteroatomic pollutants were concentrated. The naphtha cut contained aromatics in similar proportions to those found in the heavy naphthas produced in the reforming process of oil refining (reformates), but more aromatics than that of petroleum-derived naphthas used for steam cracking, which, although they can reach almost 40 wt% of aromatics, normally contain around 10 wt% [51].

Kerosene fraction was also mainly composed of aromatic hydrocarbons (56.3 wt%), being naphthalene and its derivatives the main fraction in this case, followed by styrene and cycloaromatic hydrocarbons such as indene. The content of olefins in kerosene was double that of naphtha (16.6 wt%), while saturates were in smaller proportion than in the naphtha cut (5.7 wt%). As can be seen in Table 4, the content of non-hydrocarbons in the kerosene fraction was very high (21.4 wt%), indicating that heteroatomic compounds in the pyrolysis oil were mainly concentrated in this fraction. In general terms, this kerosene fraction was very different in composition compared to traditional petroleum-derived kerosene, which usually has a much higher saturates content (≈ 55 wt%), a lower aromatic content (≈ 20 wt%) and a much lower amount of non-hydrocarbons, normally related to sulfur [53]. It is also worth mentioning the high content of naphthalenes in this kerosene fraction (18.4 wt%), much higher than the established limit for fuel purposes (3 vol% ≈ 3.5 wt%).

The atmospheric gas oil (AGO) fraction showed a composition similar to that of kerosene, with slightly higher concentrations of saturates, olefins and aromatics, i.e., a lower non-hydrocarbon content (13.4 wt%). The predominant aromatic compounds in this case were two-ring aromatics, including biphenyls (22.8 wt%) and naphthalenes (15.3 wt%), with a significant presence of triaromatics (14.6 wt%). Styrene, although still present in AGO, was in low concentration (1.1 wt %). The composition of this fraction, again, was quite different to AGO from petroleum sources [53,54]. At last, it was not possible to analyze the residue fraction due to issues derived from its high boiling point, so it is not included in the table.

3.2. Characterization of hydrotreated PWPO and hydrotreatment gases

After hydrotreatment of PWPO two products were obtained: the hydrotreated PWPO, called primary liquid, and a small fraction of gases. Primary liquid was the main product of the hydrotreating process, yielding 98.8–99.7 wt% with respect to PWPO initial mass. The characterization of the primary liquids obtained after each treatment cycle (240–270–300–330–360 °C) included measuring pollutant concentrations and quantifying distillation fractions.

Fig. 3 shows the concentration of nitrogen and sulfur (up) and chlorine and bromine (down) in the primary liquids. Halogens concentrations below the detection limit (5 mg kg^{-1}) are marked as 0 mg kg^{-1} in order to make the figure coherent. As can be seen, both catalysts exhibited similar behavior in their hydrodenitrogenation (HDN) capacity, producing liquids with lower nitrogen content as the temperature increased. The CoMo catalyst was slightly more active in HDN than NiMo catalyst at lower temperatures (240 and 270 °C), while it showed lower activity at 300 and 330 °C, which could indicate a stronger deactivation phenomenon related to the time-on-stream. The best HDN efficiency, 94.1%, was obtained with NiMo catalyst at 360 °C, resulting in a liquid with 411 mg kg^{-1} of nitrogen. A very similar HDN efficiency was reported by Yoon et al. for the batch hydrogenation of plastic-waste pyrolysis oil at 350 °C using a NiMo over alumina catalyst [32].

Regarding sulfur, it should be noted that DMDS was added to the feedstock to enhance catalyst stability. Thus, at the lowest process temperatures (240 °C and 270 °C) DMDS was yet not fully removed, resulting in a higher sulfur concentration than in the original PWPO.

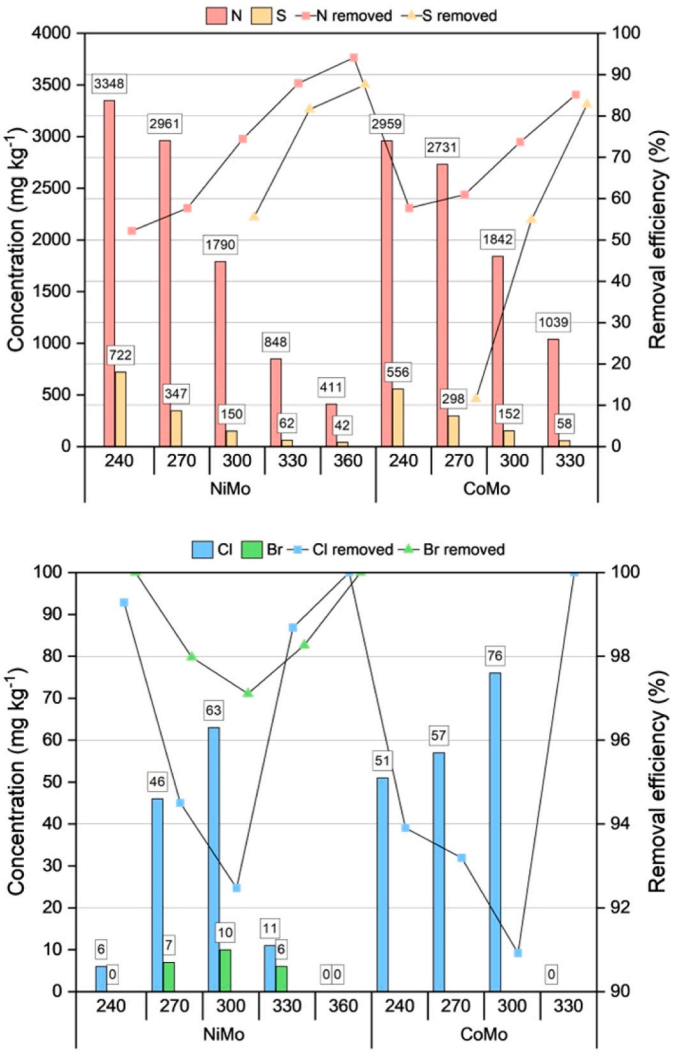


Fig. 3. Heteroatoms removal in primary liquids at different temperatures and catalysts: nitrogen & sulfur (up) and chlorine & bromine (down).

Hydrodesulfurization (HDS) could already be observed at temperatures above 300 °C, with both catalysts showing similar activity. The best result was obtained at 360 °C with the NiMo catalyst (42 mg kg^{-1} S and 87.5% removal efficiency). This removal efficiency, although similar to that reported by other authors [55], was lower than the nitrogen removal efficiency and the halogen removal efficiency (discussed below). This could be due to the presence of chlorine, which has been reported to inhibit HDS reactions [30].

The differences in the performance of the two catalysts, mainly in HDN, can be explained from the nature of their active sites. Both are associated with Co or Ni promoted MoS_2 edge structures containing sulfur vacancies and unsaturated metal centers. However, the promoter modifies the reactivity of these edge sites in different ways. Co-Mo-S phases generally exhibit a greater propensity for vacancy-mediated bond cleavage reactions, favoring the direct removal of heteroatoms through C–O, C–N, C–S and C–X (halogen) bond scission pathways. In contrast, Ni-Mo-S phases possess a higher hydrogenation functionality due to their enhanced ability to dissociate hydrogen and maintain a higher surface concentration of reactive hydrogen species [56,57].

Under relatively mild hydrotreating conditions, the superior activity of CoMo catalysts is frequently attributed to the higher effectiveness of Co-Mo-S edge sites for direct heteroatom elimination, which can proceed without extensive prior hydrogenation of the molecular structure. Such behavior is particularly advantageous for highly functionalized

pyrolysis-oil molecules, where oxygen removal and stabilization can occur through relatively low-temperature pathways. In addition, the lower hydrogenation tendency of Co-Mo-S may reduce the accumulation of strongly adsorbed partially hydrogenated intermediates, thereby maintaining a higher turnover frequency under kinetic control.

As temperature increases, the catalytic advantage progressively shifts towards NiMo catalysts. Elevated temperatures facilitate hydrogen-assisted reaction pathways involving the saturation of aromatic rings, hydrogenation of unsaturated fragments, and stabilization of radical or reactive oxygenated intermediates. The higher hydrogen activation capacity of Ni-Mo-S phases promotes routes that require multiple sequential hydrogenation–hydrogenolysis steps. Consequently, NiMo catalysts generally outperform CoMo catalysts under severe hydrotreating conditions, where the overall conversion is governed not only by heteroatom removal but also by the extensive hydrogenation and stabilization of highly condensed aromatic and heteroaromatic structures [58]. Therefore, while CoMo catalysts may exhibit superior performance at lower temperatures owing to their greater efficiency for direct heteroatom removal reactions, NiMo catalysts become increasingly advantageous as reaction severity increases because their stronger hydrogenation functionality facilitates deep upgrading of the pyrolysis-oil matrix. This transition reflects a shift in the controlling mechanism from vacancy-mediated to hydrogen-assisted conversion of complex oxygenated, nitrogenated and halogenated species.

The bottom part of Fig. 3 shows the results of hydrodehalogenation (HDX). It can be proved that the HDX activity of both catalysts were very high, given that the PWPO contained 837 mg kg^{-1} of Cl and 346 mg kg^{-1} of Br, and that the maximum concentration in the hydrotreated liquids was 76 mg kg^{-1} of chlorine (CoMo catalyst at 300 °C). In this case, a clear tendency was observed with both catalysts: high HDX activity at the lowest temperature, worse HDX activity at intermediate temperatures (270 and 300 °C) and high HDX activity again from 330 °C onwards. The maximum and virtually complete removal of halogens (halogen concentration below 5 mg kg^{-1}) was reached at 360 °C for NiMo catalyst and at 330 °C for CoMo catalyst. Bromine content could not be determined in CoMo experiments due to technical issues, but a resembling behavior that observed with NiMo catalyst is expected.

Similar observations in HDX were made in a previous study of the authors focused on the hydrotreating of mixed plastic waste pyrolysis oil rich in nitrogen and chlorine [59]. In that case, the comprehensive GC×GC-AED analysis showed that at temperatures above 240 °C, the released HCl reacted with unconverted olefins to form new halogenated compounds. Then, at temperatures above 300 °C, HDX activity surpassed the formation of new halogenated compounds, which was most likely due to almost complete olefin hydrogenation at reaction temperatures above 300 C. Another hypothesis to explain this behavior is the contribution of temperature to the dehalogenation of liquids through the cleavage of C-Cl and C-Br bonds, which occurs predominantly at temperatures around 300 °C [60–61]. Thus, the results obtained at 240 °C and 300 °C, which were very similar, could have taken place through different mechanisms. At 240 °C, dehalogenation would have proceeded mainly by catalytic hydrogenation, while at 300 °C the main mechanism would have been thermal dehalogenation. At last, the reversible deactivation of the catalysts by the formation of NH_4Cl could also have been taken part in this phenomenon. The catalysts may have been deactivated by the formation of NH_4Cl after the first experiment hours, partially recovering activity again due to the sublimation of NH_4Cl, which occurs at temperatures above 350 °C [30]. This way, the CoMo catalyst exhibited lower HDX activity than the NiMo catalyst at low temperatures, suggesting faster deactivation. However, halogen concentration below the detection limit was also achieved with this catalyst at 330 °C, even at lower temperatures than in the case of NiMo catalyst.

The obtained dechlorination efficiency is comparable with that obtained by Yoon et al., also working with NiMo/Al_2O_3 catalyst at 350 °C [32]. On the other hand, Seok et al. obtained a 96.8% dechlorination efficiency starting from a more chlorinated pyrolysis oils (7500 mg kg^{-1} Cl) and working with milder reaction conditions than those used in this work (280 °C, 3 MPa H_2, 2.5 h^{-1} WHSV) [31]. However, they needed to use a more expensive catalyst, concretely platinum over alumina. There are not PWPO hydrotreating works reporting the simultaneous elimination of chlorine and bromine. The most related investigation is that carried out by Amodio et al. concerning the hydropyrolysis of WEEE plastics in presence of Pd/Al_2O_3 catalyst, where a liquid with 55 mg kg^{-1} Cl and no Br was obtained [62]. However, this was a process quite different to the hydrotreating of oils carried out in this work, so a direct comparison is not feasible. Therefore, it can be said that in this work the virtually total elimination of chlorine and bromine of an halogenated PWPO has been achieved with a low cost catalyst, which is an outstanding result because it means overcoming the main barrier that pyrolysis oils face in order to be processed in oil refining and petrochemical facilities for base chemicals production.

Apart from the pore blockage by NH_4Cl deposition and (probably) coke formation, other deactivation mechanisms were also possible in such a complex chemical system. The HDX of the PWPO generates HCl and HBr, while HDN produces NH_3. These species may act as reversible inhibitors through competitive adsorption on the active edges of the catalysts, particularly under low-temperature conditions where adsorption phenomena is important. Such inhibition is expected to affect preferentially the hydrogenation functionality of the Ni-Mo-S phase, as its activity relies on efficient hydrogen activation and transfer at promoter-modified MoS_2 edge sites. Nevertheless, despite this temporary inhibition, the intrinsically higher hydrogenation capacity of NiMo catalysts remained sufficient to provide higher overall heteroatom removal than CoMo catalysts across the investigated conditions. At last, it must be said that catalysts were tried to maintain active by adding DMDS to PWPO and, although overall absolute trends across all measured parameters may be affected by catalyst deactivation and time-on-stream, their effect on observed trends was lower than that of the temperature increase. In this sense, the absence of catalyst characterization before and after the experiments constitutes a limitation on the present study, and it could lead to overestimate temperature effects.

Concerning the final fate of the pollutants removed from the PWPO during hydrotreatment (N, S, Cl, Br), such elements must be in the gaseous phase generated during hydrotreating, in the most probable chemical forms of the substances containing these elements under hydrogenation conditions: NH_3, H_2S, HCl and HBr, respectively. The mass balance of these pollutants, taking into account that their presence in the gaseous phase was calculated by difference, showed that the majority of these elements were removed from the hydrotreated liquids and transferred to the gaseous phase. For illustration purposes, the percentage of nitrogen removed was in the range 54–94% with NiMo catalyst and 58–85% with CoMo catalyst. In the case of chlorine, these ranges were 93–100% with NiMo catalyst and 91–100% with CoMo catalyst.

As with the original PWPO, the hydrotreated primary liquids obtained with both catalysts were distilled into naphtha (< 150 °C), kerosene (150–250 °C), atmospheric gas oil (AGO) (250–360 °C) and bottom residue (> 360 °C) fractions. Fig. 4 shows the distillation yields as a function of the catalyst used and temperature, all of them referred to the primary liquids yield (not absolute yields based on the PWPO feed). In the case of the NiMo catalyst, the hydrotreatment at 240 °C caused a decrease in the light fractions (naphtha and kerosene) and the equivalent increase of the heavy fractions (AGO and residue) in comparison to the PWPO (42.6 vs 49.0, 16.4 vs 22.0, 15.7 vs 10.8, 22.8 vs 16.8, respectively, in wt%). However, as the temperature rose, there was an increase in the yield of light fractions to the detriment of heavy fractions, probably induced by hydrocracking reactions promoted by the higher temperatures and the nickel-based catalyst [55]. This had a predominant impact in the naphtha fraction obtained at 360 °C, which almost reached the naphtha content of the original PWPO (48.0 vs 49.0 wt%). CoMo catalyst showed similar results in terms of fraction yields but with a difference worth mentioning: no increase in naphtha fraction was observed with rising temperature. The explanation could lie on the fact

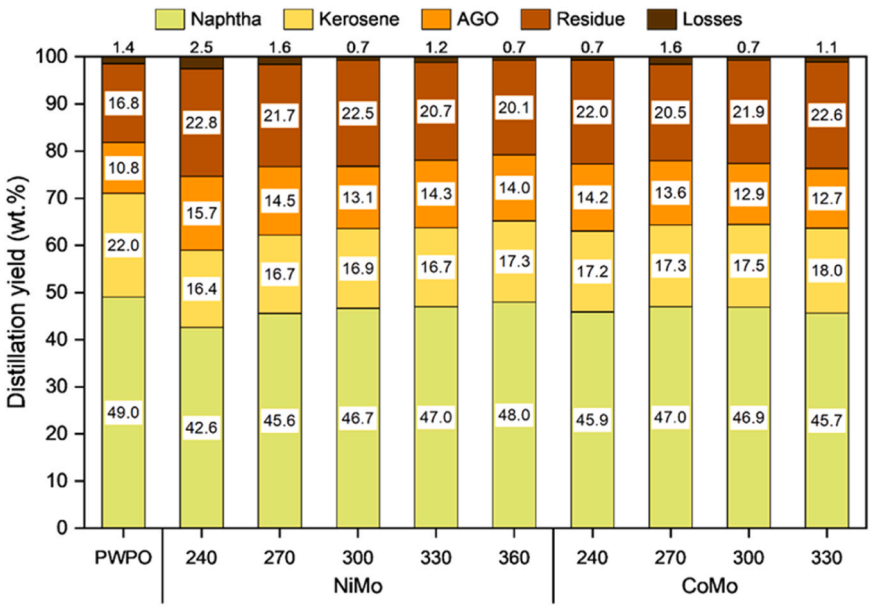


Fig. 4. Distillation cuts of hydrotreated liquids obtained at different temperatures with NiMo catalyst and CoMo catalyst.

that $CoMo/Al_2O_3$ catalysts have less hydrocracking activity than $NiMo/Al_2O_3$ catalysts [63].

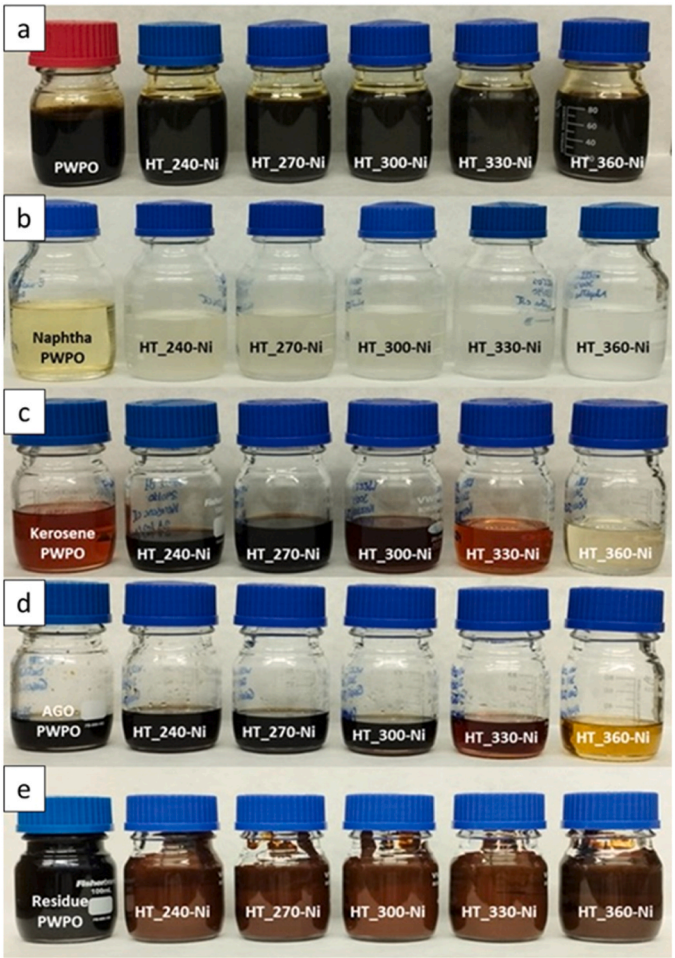


Fig. 5. Hydrotreated liquids obtained at different temperatures with NiMo catalyst. PWPO and primary liquids (a), naphtha (b), kerosene (c), AGO (d) and residue (e) cuts.

Fig. 5 shows a picture of the primary liquids, as well as the distillation cuts of these primary liquids, obtained with NiMo catalyst at different temperatures. The same picture of the hydrotreated liquids obtained with CoMo catalyst is presented in Supplementary Information document as Figure S2. It can be seen that primary liquids maintained a dark brown color, similar to the ASTM D1500–12 color of the PWPO (7.5–8.0), while the distillation cuts showed, in general terms, a color palette ranging from transparent or pale yellow for the lighter fractions to various shades of brown for the heavier fractions. In other words, the color became darker from light to heavy fractions, which is a well-known fact in oil refining [42].

The hydrotreated naphtha fractions showed a colorless appearance, out of the color scale of ASTM D1500 standard, i.e., < 0.5, and clearer than the naphtha cut of the original PWPO, which was around 0.5–1 ASTM D1500–12 color. In this case, the ASTM D156–15 Saybolt color should be determined in order to classify the color-based quality of the naphtha fractions, but, anyway, it was quite clear at a glance that the quality of the naphtha was increasing as the temperature of the hydrotreating increased. On the other hand, it was quite surprising to find that the color of the non-hydrogenated kerosene fraction was clearer than that of the low-temperature hydrogenated kerosene fractions, which was probably related with a dilution of the non-hydrogenated kerosene by non-distilled styrene in PWPO initial fractionation, due to the high concentration of styrene. Unlike what happened with naphtha, in this case there was a clear change in the color of kerosene as the temperature of hydrotreating increased with both catalysts. NiMo catalyst produced kerosene with 7.0–8.0 ASTM D1500–12 color at 240 °C and 270 °C, 6.0–7.0 at 300 °C, 3.5–4.5 at 330 °C and 0.5 at 360 °C. In the case of CoMo catalyst, the kerosene maintained the 7.0–8.0 color up to 300 °C, decreasing to 6.0–7.0 at 330 °C. In the case of AGO fractions, NiMo catalyst produced AGO with 7.0–8.0 ASTM D1500–12 color at 240–300 °C, 3.5–4.5 at 330 °C and 2.0–3.0 at 360 °C, while the AGO obtained with CoMo catalyst maintained the 7.0–8.0 color up to 300 °C, decreasing to 6.0–7.0 at 330 °C. The residue fractions presented a very similar color with both NiMo and CoMo catalysts at all the tested temperatures, corresponding to 6.0–6.5 in the color scale of the ASTM D1500–12 standard. The clearer color could be indicative of the presence of high molecular weight substances in the solid state and, consequently, it resembled the bottom fractions obtained from the distillation of polyethylene-derived pyrolysis oils [64].

Apart from primary liquids, a gas fraction was also obtained in the

hydrotreating experiments, whose composition (referred to gas yield) is shown in Fig. 6. It has to be mentioned that this composition was calculated in a basis free of gaseous forms of chlorine, bromine, nitrogen and sulfur, as well as in hydrogen-free basis, since this compound was the reactive gas of the process. As it can be seen, the main identified substances in gases were methane, ethane and propane, being propane the main substance of the NiMo experiment and methane in the case of CoMo catalyst. Ethane, n-butane, iso-butane and small quantities of butenes were also detected in the gases.

At last, the overall mass balance of the hydrotreating process with respect to the initial PWPO is presented in Fig. 7. As it can be seen, naphtha was the primary product of the process, yielding almost 50 wt% of the products, followed by the residue and kerosene fractions. The gas fraction was very minority in yield, ranging from 0.3 to 1.2 wt%, the maximum obtained at 360 °C with NiMo catalyst.

3.3. Characterization of naphtha fractions

The composition of the naphtha fractions is presented in Fig. 8, divided into saturates, olefins, aromatics and non-hydrocarbons. The aromatic hydrocarbons, the most abundant chemical family, are shown substance by substance. The so-called "PWPO" column represents the composition of the naphtha fraction of the original pyrolysis oil. Firstly, it must be said that the results obtained with the two catalysts were quite similar. In general terms, the tendency in chemical families with increasing temperature was to obtain more saturated hydrocarbons (saturates), less olefins, slightly less aromatic hydrocarbons and less non-hydrocarbons with both catalysts. The best results were obtained at 360 °C with NiMo catalyst, which produced almost 20 wt% of saturates (7.8 wt% in original naphtha cut), 2 wt% of olefins (8.4 wt% in original naphtha cut), 78.5 wt% of aromatic hydrocarbons (79.7 wt% in original naphtha cut) and 200 mg kg^{-1} of non-hydrocarbons (4.2 wt% in original naphtha cut). The decrease in olefin concentration, which are undesirable due to their reactive nature, is one of the strengths of hydrotreatment and it has been also reported to take place effectively with PWPO in other studies [65,66]. This result and the almost complete removal of non-hydrocarbons were of significant success.

In terms of individual chemicals, the most notable hydrogenation phenomenon was the complete conversion of styrene, which was not detected in any of the hydrotreated naphtha fractions. This was a very important result, as the presence of styrene in pyrolysis oils is associated with chemical instability, due to its tendency to polymerize and, consequently, form gums or solid phases that cause issues during storage and processing [15]. The disappearance of styrene was completely linked to the increase in the proportion of ethylbenzene in hydrogenated naphthas, suggesting that the conversion of styrene was directly related to its hydrogenation reaction to produce ethylbenzene. This phenomenon highlighted the high reactivity of the styrene double bond for hydrogenation compared to double bonds in non-aromatic olefins, which did not show complete hydrogenation under any of the conditions studied. The high conversion of styrene during hydrotreating has been also observed by other authors and it has been attributed to the increased electron density of the double bond of styrene, which makes it interact stronger with the active phase of the catalysts [67].

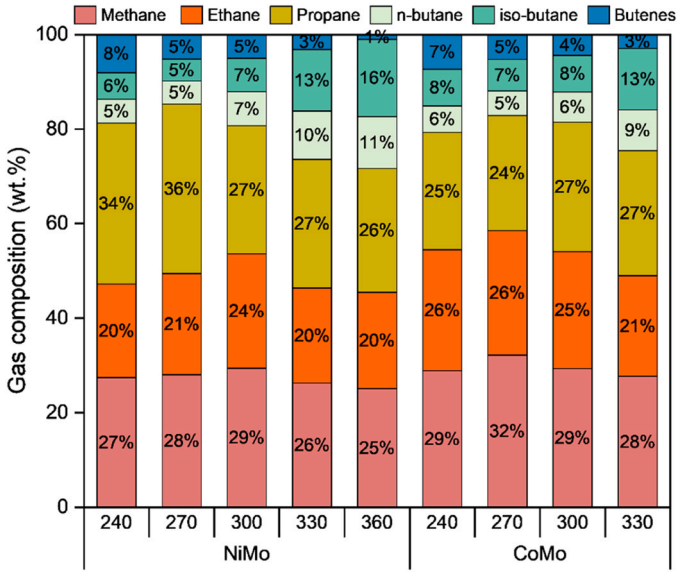


Fig. 6. Yield of the gaseous compounds generated from the hydrotreating of PWPO.

All the hydrotreated naphthas yielded BTEX concentrations (benzene, toluene, ethylbenzene and xylenes) between 74.9 and 77.8 wt%, much higher than that of the naphtha distilled from the original PWPO (43.7 wt%, see Table 2). Given this composition, the depolluted naphtha (that obtained at 360-NiMo) could be a high value-added product as raw material to produce aromatic hydrocarbons. In the traditional process of obtaining aromatics in refineries, the raw material is the so-called reformate, i.e., the product of catalytic reforming of heavy naphtha [68]. This product is also a mixture of hydrocarbons that can contain a concentration of aromatics like the naphtha obtained in this work, as well as very similar proportions of benzene and toluene [69]. The aromatic hydrocarbons in the reformate are separated from the rest of the hydrocarbons by solvent extractive distillation [70]. The solvent is then recovered and the aromatics are fractionated into benzene, toluene and xylenes (BTX). The naphtha obtained in this work could follow the same route, producing benzene, toluene and ethylbenzene as a third product, where the o-xylene would be also present in a concentration around 2.5 wt%. These substances are used in the manufacture of plastics such as polyurethane, polyamide, polycarbonates, polystyrene, etc. Therefore, the hydrotreated naphtha obtained in this work at 360-NiMo could be of interest for the design of circular strategies in the production of plastics.

Table 3 shows the density, nitrogen concentration and sulphur concentration of the obtained naphthas in comparison with the naphtha fraction of the raw PWPO. Density did not change significantly across the different temperatures in both experiments; only a slight decrease in density was observed with increasing temperature, likely due to a decrease in aromatic hydrocarbons. The observed difference of density between the naphtha distilled from the original PWPO and the hydrotreated naphthas can be associated with the content of styrene and ethylbenzene in both kinds of samples. In terms of comparison, although the density of the hydrotreated naphthas was lower than that of the original PWPO, it was still higher than the specification for fossil-based naphthas, which is 0.66–0.72 g cm^{-3}. The disparity in density is logical considering that fossil-based naphthas are products with very low aromatic hydrocarbon content [51].

Regarding nitrogen and sulfur, both catalysts showed a decreasing trend in pollutant concentration with increasing temperature, as reported above for the primary liquids. Hydrotreating at 360 °C with a NiMo catalyst produced naphtha with N and S concentrations below the equipment's quantification limit of 10 mg kg^{-1}. It should be remembered that the primary liquids obtained at these conditions had less than 5 mg kg^{-1} of chlorine and bromine (Fig. 3). Thus, this means that under such hydrogenation conditions, a virtual N, S and halogen-free naphtha was obtained. Considering that the total measured concentration of non-hydrocarbons in this experiment was 200 mg kg^{-1}, it could be concluded that this concentration mainly referred to oxygenated compounds, and consequently, the elemental oxygen concentration was also very low. This was again a good result since oxygen is related to chemical instability and corrosion potential of pyrolysis oils [14].

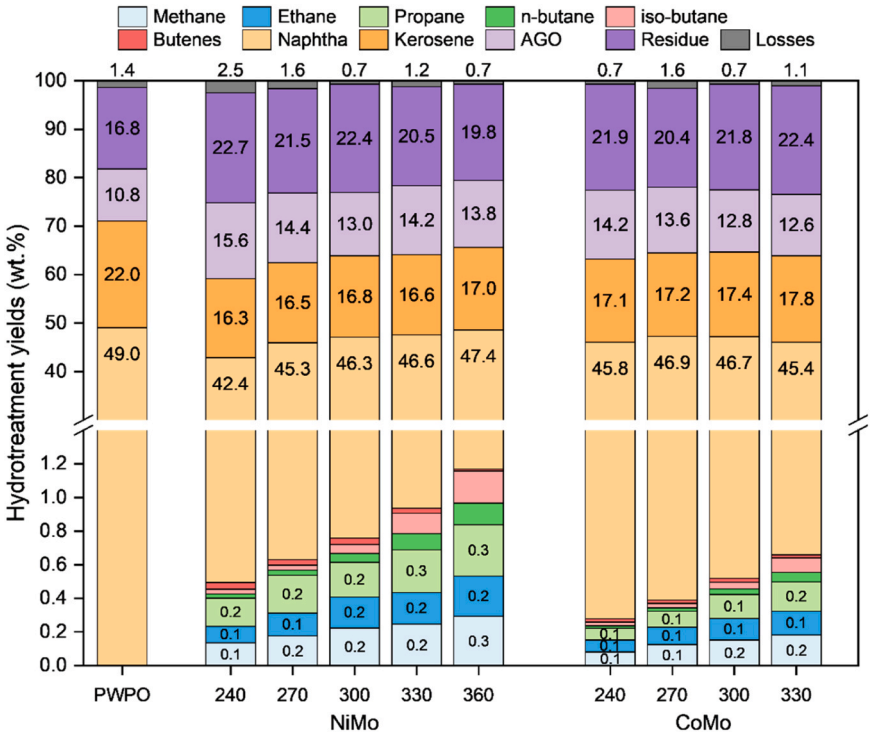


Fig. 7. Overall mass balance of the hydrotreating process.

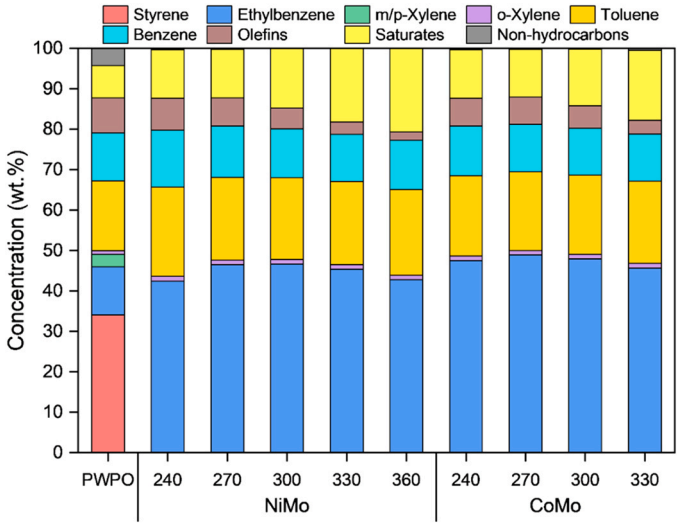


Fig. 8. Composition (wt%) of naphtha fractions.

3.4. *Characterization of kerosene fractions*

The composition of the kerosene fractions is presented in Fig. 9, divided into non-hydrocarbons, saturates, olefins and aromatic hydrocarbons. The aromatic hydrocarbons, the most abundant group, are subdivided into naphthalenes, cycloaromatics, alkylbenzenes and styrene. Again, the "PWPO" column represents the composition of the kerosene fraction of the original pyrolysis oil. As in the case of naphthas, the results obtained for kerosene fractions with the two catalysts were quite similar. The hydrotreating at 240 °C resulted in a significant increase in saturates content, from 5.7 wt% in the non-hydrotreated kerosene to 22.7 wt% in the hydrotreated kerosene with NiMo catalyst and 21.8 wt% in the hydrotreated kerosene with CoMo catalyst. This can be attributed to the hydrogenation of olefins, which decreased from 16.6 wt% to 9.3 wt% (NiMo) and 10.3 wt% (CoMo), and the hydrogenation of the non-hydrocarbons, which decreased from 21.4 wt% to 5.0 wt% (NiMo) and 7.2 wt% (CoMo). At 240°C, both catalysts were also able to eliminate almost all the styrene in the kerosene fraction to produce ethylbenzene. The increase in naphthalenes during hydrotreatment (from 18.4 wt% to 24.6 wt% with NiMo and 24.4 wt% with CoMo) could be related to the elimination of heteroatoms from non-hydrocarbons, mainly heteroatomic naphthalene compounds. Other authors have also reported the formation of aromatics during hydrotreating of pyrolysis oils [71–72].

From 240 °C onwards, more saturates were produced, with decreasing amounts of olefins and non-hydrocarbons for both catalysts. However, the total aromatic content did not show significant changes with increasing temperature, but they could be appreciated within the different groups of aromatics identified. With the NiMo catalyst, increasing temperature led to more cycloaromatics at the expense of naphthalenes, indicating hydrogenation of the latter. This phenomenon did not occur over the CoMo catalyst, pointing out lower hydrogenation capacity. The best results were obtained again at 360 °C with NiMo

Table 3
Other properties of naphtha fractions.

	Density at 15 °C (kg m^{-3})	Total N (mg kg^{-1})	Total S (mg kg^{-1})
PWPO	861.5	3200	119
HT_240-Ni	841.6	372	193
HT_270-Ni	843.1	206	128
HT_300-Ni	840.9	73	40
HT_330-Ni	837.7	36	20
HT_360-Ni	833.9	< 10	< 10
HT_240-Co	843.7	203	109
HT_270-Co	843.9	238	69
HT_300-Co	841.4	115	31
HT_330-Co	838.6	50	12

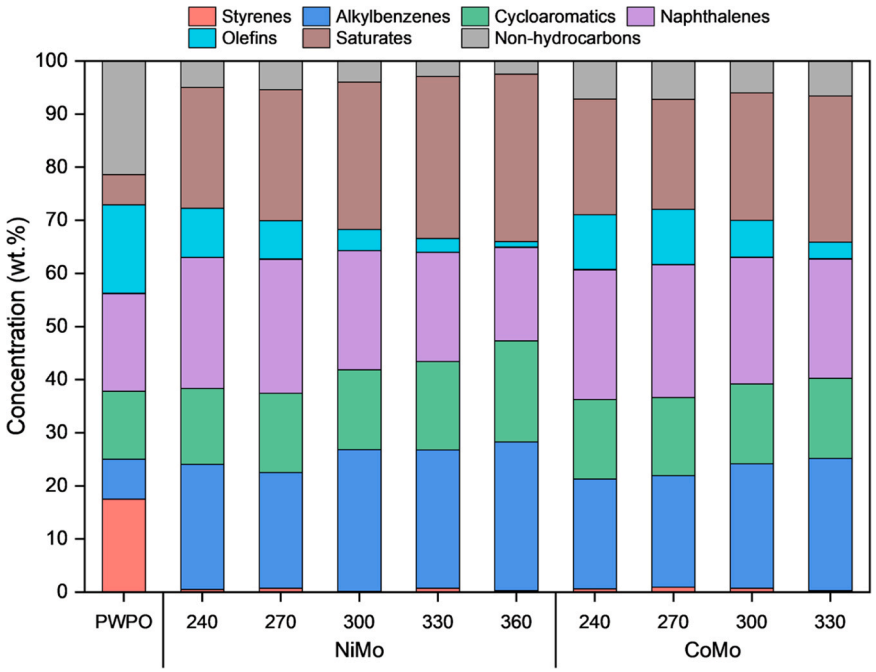


Fig. 9. Composition (wt%) of kerosene fractions.

catalyst, which produced 31.5 wt% of saturates (5.7 wt% in original kerosene cut), 1 wt% of olefins (16.6 wt% in original kerosene cut), 65 wt% of aromatics (56.3 wt% in the original kerosene cut) and 2.5 wt % of non-hydrocarbons (21.4 wt% in original kerosene cut). In this case, it should be noted that the hydrogenation efficiency of this fraction was very high, obtaining kerosene with fewer olefins and more saturates than the naphtha obtained under the same conditions, and being able to reduce the presence of non-hydrocarbons by 19 %age points.

Some other properties of the kerosene fractions are reported in Table 4, namely, density, kinematic viscosity, total nitrogen and total sulfur. Density showed a decreasing tendency with increasing temperature, more pronounced with NiMo catalyst, maybe related this time to the decrease of non-hydrocarbons and increase of saturates, since total aromatics remained approximately constant. These densities were higher than the specification for JET A−1 kerosene, which must be lower than 840 kg m^{-3} [33]. On the other hand, kinematic viscosity did show a clear decreasing tendency with increasing temperature when working with NiMo catalyst. This was also true for CoMo catalyst but surprisingly the kinematic viscosity of the kerosene fractions obtained from 240 to 300 °C was higher than that of the non-hydrotreated kerosene, probably caused by the increasing of the content of linear alkanes. Taking into account that the specification for JET A−1 kinematic viscosity at −20 °C requires it to be lower than 8 $mm^2 s^{-1}$, most of the kerosene fractions met the limit. Concerning contents of nitrogen and sulfur, they showed a clear decreasing tendency as temperature was increased with both catalysts, reaching 86 mg kg^{-1} of N and 17 mg kg^{-1} of S after hydrotreating at 360 °C with NiMo catalyst. The sulfur content also met the specification of 3000 mg kg^{-1}, while nitrogen, although not included in the specifications, was low enough to avoid issues related to it. Besides, it should be remembered again that the primary liquids obtained at these conditions contained less than 5 mg kg^{-1} of chlorine and bromine (Fig. 3).

Table 4
Other properties of kerosene fractions.

	Density at 15 °C (kg m^{-3})	Kinematic viscosity at −20 °C ($mm^2 s^{-1}$)	Total N (mg kg^{-1})	Total S (mg kg^{-1})
PWPO	910.9	7.2	7143	429
HT_240-Ni	899.7	5.9	3210	1129
HT_270-Ni	894.8	5.6	513	603
HT_300-Ni	890.0	5.2	285	173
HT_330-Ni	885.1	4.4	129	44
HT_360-Ni	880.5	4.2	86	17
HT_240-Co	895.0	10.2	2440	216
HT_270-Co	892.8	9.0	2604	389
HT_300-Co	890.9	7.9	1684	129
HT_330-Co	889.5	5.3	893	54

Concerning applications, the high aromatic content of the best kerosene (obtained at 360-NiMo) means it does not comply with JET A−1 fuel specifications, especially regarding naphthalene content, which must be less than or equal to 3 vol%, whereas the fuel obtained in this study contained 17.6 wt% (15.5 vol%). However, this kerosene could be an interesting source for the production of sustainable aviation fuel (SAF), since the usual source of SAF, synthetic paraffinic kerosene (SPK) obtained from vegetable oil, does not contain enough aromatic hydrocarbons to reach the typical values of aviation kerosene [73]. Therefore, mixing SPK with this aromatic kerosene could produce a high-quality SAF. On the other hand, the same high naphthalene content makes this kerosene a product similar to naphthalene oil, which is produced by distillation of coal tar [74]. Among the uses of this oil is the production of phthalic anhydride, which in turn is used in the manufacture of plastics and resins. Therefore, this application would also make it possible for the kerosene fraction of hydrotreated pyrolysis oil to be used in a circular production scheme for plastics.

3.5. Characterization of atmospheric gas-oil (AGO) fractions

The compositional analysis of AGO showed that aromatic hydrocarbons, the most abundant family, consisted primarily of naphthalenes, biphenyls and triaromatics (Fig. 10). As in the previous sections, the

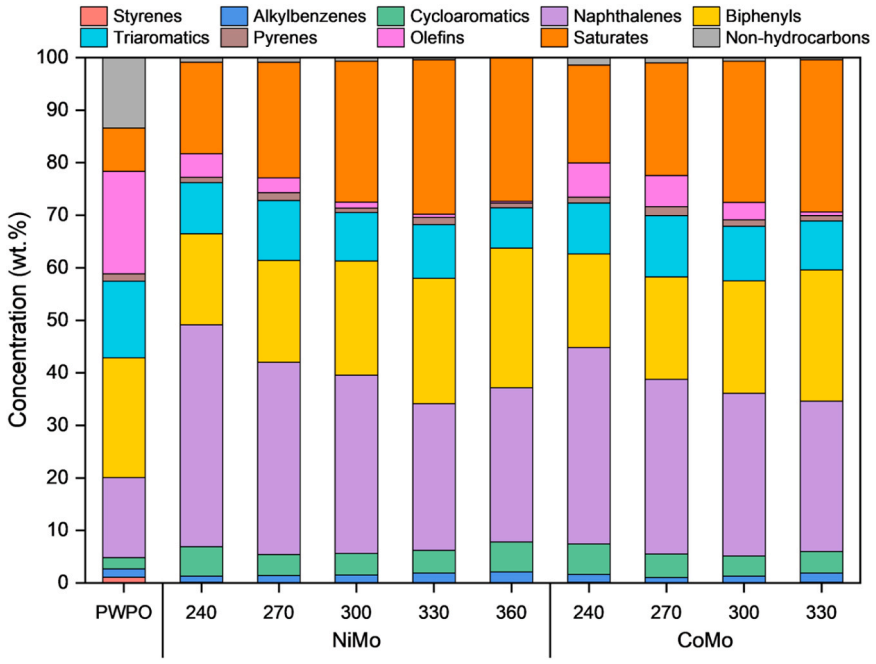


Fig. 10. Composition (wt%) of AGO fractions.

"PWPO" column in Fig. 10 represents the composition of the AGO fraction of the original pyrolysis oil. The AGO fractions obtained with the two catalysts were quite similar, with slightly better results from the NiMo catalyst. As was the case with naphthas and kerosenes, a significant increase in saturates content (more than two-fold compared to non-hydrotreated AGO) was observed after the hydrotreating at 240 °C. This was the primary consequence of the hydrogenation of olefins (decreasing from 19.5 wt% to 4.5 wt% and 6.5 wt% with NiMo and CoMo, respectively). At 240°C, the content of naphthalenes increased, specifically from 15.3 wt% to 42.2 wt% (NiMo) and 37.4 wt% (CoMo). This was caused primarily by naphthalene formation from triaromatics (decrease by one third) and non-hydrocarbons (decrease by 90%). A decrease in concentration was also observed for biphenyls (from 22.8 wt % to 17.3 wt% and 17.8 wt% with NiMo and CoMo, respectively). Further increases in temperature, up to 360 °C, resulted in higher concentrations of saturates and biphenyls, while reducing olefins, naphthalenes and non-hydrocarbons for both catalysts. Considering that the absolute priority for all the distilled fractions in this work is the removal of heteroatoms, the best results were obtained at 360 °C with NiMo catalyst. The AGO produced at these operational conditions contained 200 ppm of non-hydrocarbons, 27.4 wt% of saturates, 0.3 wt% of olefins, and 72.3 wt% of aromatics. AGO was, therefore, the distillation cut with the lowest olefin content.

As in previous cases, decreases in density, kinematic viscosity, and total nitrogen and sulfur concentrations were observed as the hydrotreatment conditions became more severe (Table 5). Concerning density and nitrogen content, the lowest values obtained (927.7 kg m^{-3} and 571 mg kg^{-1}) were higher than typical values of fossil AGO. However, kinematic viscosity was in the range of viscosity of fossil AGO fractions (2–4.5 mm^2 s^{-1}) and sulfur was significantly lower than the typical sulfur content of this distillation cut of petroleum [75–76].

Regarding the possible valorization options, AGO contained significantly more aromatic hydrocarbons than gas-oils from crude oil distillation [53], and, as it is clear from all parameters above, blending with diesel fuel will be significantly restricted to units of percent, primarily due to the polyaromatic content. However, AGO presented quite a similar profile to light cycle oil (LCO) in total content of aromatics and total content of di-aromatics [77]. LCO is a valuable feedstock for BTX production, which, as said above, are relevant raw materials for plastic production. Besides, this AGO contained higher naphthalene content than the kerosene fraction, being therefore again a product similar to naphthalene oil from the distillation of coal tar. At last, this fraction could also be further hydroprocessed in oil refineries in a waste-refinery-based scheme [78].

Table 5
Other properties of AGO fractions.

	Density at 15 °C (kg m^{-3})	Kinematic viscosity at 40 °C (mm^2 s^{-1})	Total N (mg kg^{-1})	Total S (mg kg^{-1})
PWPO	958.4	5.3	11051	965
HT_240-Ni	940.9	4.7	4631	1183
HT_270-Ni	939.1	4.8	3824	515
HT_300-Ni	931.0	4.1	2555	212
HT_330-Ni	927.7	4.2	1205	107
HT_360-Ni	929.2	3.8	571	57
HT_240-Co	937.9	4.5	5497	730
HT_270-Co	936.4	4.9	4957	473
HT_300-Co	930.2	4.4	3411	287
HT_330-Co	928.7	4.2	1839	112

3.6. *Characterization of residue fractions*

Table 6 presents the characterization of the residue fractions in terms of saturate compounds content and sulfur and nitrogen concentration, the only properties that could be analyzed due to the nature of this fraction. As it can be seen, the increase of the process temperature enhanced the hydrogenation of the species present in the residue fraction with both catalysts, augmenting the content of saturate compounds up to 24.8% (HT_330-Ni). On the other hand, higher temperatures and hydrogenation rates reduced the concentration of heteroatomic

Table 6
Properties of residue fractions.

	Total saturates (wt%)	Total N (mg kg^{-1})	Total S (mg kg^{-1})
HT_240-Ni	12.3	4326	1184
HT_270-Ni	15.5	4131	382
HT_300-Ni	21.5	3974	129
HT_330-Ni	24.8	1949	67
HT_360-Ni	23.6	995	38
HT_240-Co	15.0	7540	643
HT_270-Co	15.3	6008	330
HT_300-Co	19.0	4379	176
HT_330-Co	23.7	2583	84

compounds in the residue fraction. NiMo catalyst demonstrated better denitrogenation efficiencies than those of the CoMo catalyst, obtaining the lowest nitrogen concentration with this catalyst at 360 °C (995 mg kg^{-1}). Sulfur, whose initial concentration was conditioned by the addition of sulfur compounds for the activation of the catalyst, decreased its concentration below 100 mg kg^{-1} at the highest process temperatures. The lowest sulfur concentration, 38 mg kg^{-1}, was obtained with the NiMo catalyst at 360 °C.

The most realistic utilization option in terms of recycling of the so-called waste plastic oil residue (also called pyrolytic bitumen in some publications) is the blending with other heavy fractions to produce products such as heating oil, marine fuel or bitumen. In a recent work published by Schlehöfer et al., the compatibility of the pyrolytic bitumen with traditional feedstock of hydrocracking and fluid catalytic cracking (FCC) processes was evaluated. The best homogeneity and compatibility were observed at 10 wt% blending, being the combination with feed for hydrocracking the most suitable for waste plastics pyrolysis oil residue [79]. Therefore, the possibility of a hydrocracking upgrading process for the residue fractions can be a solution to produce more naphtha from PWPO.

4. Conclusion

The main conclusions drawn from this work are as follows:

- ✓ Hydrotreatment at temperatures of 330–360 °C is an effective process for upgrading olefin-rich pyrolysis oils contaminated with heteroatoms such as nitrogen, sulfur, oxygen, chlorine and bromine.
- ✓ The NiMo catalyst has been found to be more efficient in removing olefins and heteroatoms, as well as in maximizing the naphtha fraction, than the CoMo catalyst.
- ✓ The best results were obtained with the NiMo catalyst at 360 °C, producing:
  - o 48 wt% of halogen free naphtha fraction (< 150 °C), containing < 10 mg kg^{-1} N, < 10 mg kg^{-1} S, 2 wt% of olefins, and 73 wt% of BTEX.
  - o 17.3 wt% of halogen free kerosene fraction (150–250 °C), containing 86 mg kg^{-1} N, 17 mg kg^{-1} S, 1 wt% olefins, and 17.6 wt% naphthalenes.
  - o 14.0 wt% of halogen free gas oil fraction (250–360 °C), containing 571 mg kg^{-1} N, 57 mg kg^{-1} S, 0.3 wt% olefins, and 29.4 wt% naphthalenes.
  - o 20.1 wt% of halogen free heavy fraction (> 360 °C).
- ✓ The distilled fractions obtained open possibilities for material recycling of the hydrotreated oil:
  - o The naphtha cut could be used as a raw material for the separation of benzene, toluene, and ethylbenzene, to be used in the formulation of plastics such as polyurethane, polyamide, polycarbonates, polyethylene terephthalate or polystyrene with recycled content.
  - o Kerosene and gas oil cuts could be mixed with naphthalene oil for the production of phthalic anhydride used in the manufacture of resins with recycled content.
  - o The heavy fraction should be analyzed in greater depth, but unless it is hydrocracked to lighter cuts, it may serve directly as an alternative marine fuel, heating oil or in the manufacture of bitumen.

Future research should focus on two main aspects: (1) adjusting distillation temperatures to maximize the BTEX content in the naphtha fraction and concentrate all naphthalene and its derivatives in a single fraction, and (2) a comprehensive analysis of the heavy fraction in order to establish the most perspective applications.

CRediT authorship contribution statement

Alexander Lopez-Urionabarrenechea: Writing – review & editing, Writing – original draft, Funding acquisition, Conceptualization. **Petr Straka:** Writing – review & editing, Validation, Supervision, Resources, Methodology, Investigation, Data curation, Conceptualization. **Borja Baltasar Perez-Martinez:** Writing – review & editing, Writing – original draft, Resources, Investigation, Funding acquisition, Data curation, Conceptualization. **Miloš Auersvald:** Writing – review & editing, Investigation, Formal analysis. **Dan Vrtiška:** Writing – review & editing, Validation, Investigation.

Declaration of Competing Interest

The authors declare that they have no known competing financial interests or personal relationships that could have appeared to influence the work reported in this paper.

Acknowledgements

The authors want to thank the financial support to carry out this investigation to the Basque Government (consolidated research groups, IT1554–22), the University of the Basque Country (predoctoral research staff recruitment grant, PIF21/296, and doctoral candidates mobility grant, MOV23/39) and the Ministry of Education, Youth, and Sports of the Czech Republic from the institutional support of the research organization (CZ60461373). Besides, the authors thank for the technical support provided by the general services of the University of the Basque Country (SGIker) in the analysis of elemental oxygen. At last, the authors are also grateful to Nantek company, for supplying pyrolysis oils.

Appendix A. Supporting information

Supplementary data associated with this article can be found in the online version at doi:10.1016/j.jece.2026.124229.

Data availability

Data will be made available on request.

References

[1] Plastics Europe. The Circular Economy for Plastics. A European Analysis (2024). https://plasticseurope.org/knowledge-hub/the-circular-economy-for-plastics-a-european-analysis-2024/ (accessed on 14th May 2026).
[2] X. Shi, Z. Chen, L. Wu, W. Wei, B.J. Ni, Microplastics in municipal solid waste landfills: Detection, formation and potential environmental risks, Curr. Opin. Environ. Sci. Health 31 (2023) 100433, https://doi.org/10.1016/j.coesh.2022.100433.
[3] P. Yuan, X. Cao, L. Zhao, X. Xu, A. Romero-Freire, H. Qiu, Overlooked yet critical pathways for microplastics input to soil and groundwater system: transport mechanisms and simulation predictions in landfill environments, Water Res. 284 (2025) 124041, https://doi.org/10.1016/j.watres.2025.124041.

[4] B. Hegedüs, Á.B. Palotás, G. Muránszky, Z. Dobó, Investigation of gasoline-like transportation fuel obtained by plastic waste pyrolysis and distillation, J. Clean. Prod. 447 (2024) 141500, https://doi.org/10.1016/j.jclepro.2024.141500.
[5] M. Laghezza, S. Fiore, F. Berruti, A review on the pyrolytic conversion of plastic waste into fuels and chemicals, J. Anal. Appl. Pyrolysis 179 (2024) 106479, https://doi.org/10.1016/j.jaap.2024.106479.
[6] G. Ragonnaud, 2025. Circularity requirements for vehicle design and management of end-of-life vehicles. European Parliament. Available online: https://www.europarl.europa.eu/thinktank/en/document/EPRS_BRI(2023)754627 (accessed on 14th May 2026).
[7] M. Kusenberg, A. Eschenbacher, M.R. Djokic, A. Zayoud, K. Ragaert, S. De Meester, K.M. Van Geem, Opportunities and challenges for the application of post-consumer plastic waste pyrolysis oils as steam cracker feedstocks: To decontaminate or not to decontaminate? Waste Manag. 138 (2022) 83–115, https://doi.org/10.1016/j.wasman.2021.11.009.
[8] M. Kusenberg, M. Roosen, A. Zayoud, M.R. Djokic, H.D. Thi, S.De Meester, K. Ragaert, U. Kresovic, K.M.Van Geem, Assessing the feasibility of chemical recycling via steam cracking of untreated plastic waste pyrolysis oils: Feedstock impurities, product yields and coke formation, Waste Manag. 141 (2022) 104–114, https://doi.org/10.1016/j.wasman.2022.01.033.
[9] A. Karaba, T. Anh Le, J. Patera, M. Suková, R. Suchopa, T. Herink, P. Zámostný, Waste plastic pyrolysis oils are promising feedstock for sustainable monomers production via steam cracking process, J. Anal. Appl. Pyrolysis 186 (2025) 106950, https://doi.org/10.1016/j.jaap.2025.106950.
[10] A. Serras-Malillos, B.B. Perez-Martinez, A. Iriondo, E. Acha, A. Lopez-Urionabarrenechea, B.M. Caballero, Quantification of the composition of pyrolysis oils of complex plastic waste by gas chromatography coupled with mass spectrometer detector, RSC Adv. 14 (2024) 9892, https://doi.org/10.1039/d4ra00226a.
[11] L. Esposito, L. Cafiero, D. De Angelis, R. Tuffi, S.V. Ciprioti, Valorization of the plastic residue from a WEEE treatment plant by pyrolysis, Waste Manag. 112 (2020) 1–10, https://doi.org/10.1016/j.wasman.2020.05.022.
[12] L.S. Stefano, L. Cafiero, D. De Angelis, S. Pavoni, R. Tuffi, M. Scarsella, Thermal pyrolysis of a real plastic sample from small WEEE and characterization of the produced oil in view of fuel or feedstock uses, Therm. Sci. Eng. Prog. 48 (2024) 102403, https://doi.org/10.1016/j.tsep.2024.102403.
[13] B.B. Perez-Martinez, A. Lopez-Urionabarrenechea, A. Serras-Malillos, E. Acha, M. Martínez-Santos, B.M. Caballero, M. Iturrondobeitia, H. Afonso, Recycling of plastic-rich streams from waste electrical and electronic equipment (WEEE) sorting plants: An in-depth study of pyrolysis potential through product characterization and life cycle assessment (LCA), Energy Conv. Manag. 329 (2025) 119633, https://doi.org/10.1016/j.enconman.2025.119633.
[14] W. Zeb, M. Roosen, P. Knockaert, S. Janssens, D. Withoeck, M. Kusenberg, J. Hogie, P. Billen, S. Tavernier, K.M. Van Geem, S. De Meester, Purification and characterisation of post-consumer plastic pyrolysis oil fractionated by vacuum distillation, J. Clean. Prod. 416 (2023) 137881, https://doi.org/10.1016/j.jclepro.2023.137881.
[15] S. Cañete, L. Faba, S. Ordoñez, Continuous hydrogenation of plastic wastes pyrolysis oil over used hydrotreatment catalysts, Catal. Today 454 (2025) 115308, https://doi.org/10.1016/j.cattod.2025.115308.
[16] I. Hita, A.T. Aguayo, M. Olazar, M.J. Azkoiti, J. Bilbao, J.M. Arandes, P. Castaño, Kinetic Modeling of the Hydrotreating and Hydrocracking Stages for Upgrading Scrap Tires Pyrolysis Oil (STPO) toward High-Quality Fuels, Energy Fuels 29 (2015) 7542–7553, https://doi.org/10.1021/acs.energyfuels.5b01502.
[17] S. Bezergianni, A. Dimitriadis, G.C. Faussone, D. Karonis, Alternative Diesel from Waste Plastics, Energies 10 (2017) 1750, https://doi.org/10.3390/en10111750.
[18] F. Faisal, M.G. Rasul, A.A. Chowdhury, D. Schaller, M.I. Jahirul, Uncovering the differences: A comparison of properties of crude plastic pyrolytic oil and distilled and hydrotreated plastic diesel produced from waste and virgin plastics as automobile fuels, Fuel 350 (2023) 128743, https://doi.org/10.1016/j.fuel.2023.128743.
[19] S. Rodríguez, R. Palos, I. Crespo, J. Bilbao, J.M. Arandes, A. Gutiérrez, Suitable properties of the HY zeolite of NiW/HY catalysts for the hydroprocessing of a plastic pyrolysis oil/vacuum gas oil (PPO/VGO) blend, J. Anal. Appl. Pyrolysis 186 (2025) 106910, https://doi.org/10.1016/j.jaap.2024.106910.
[20] P. Kokayeff, S. Zink, P. Roxas, Hydrotreating in Petroleum Processing, in: S. A. Treese, David S. Jones, P.R. Pujado (Eds.), Handbook of Petroleum Processing, Springer, Switzerland, 2014, pp. 361–434, https://doi.org/10.1007/978-3-319-05545-9_4-1.
[21] J.G. Speight. Hydrotreating and Hydrocracking Processes in Refining Technology, first edition, CRC Press, Boca Ratón, Florida, 2023, https://doi.org/10.1201/9781003185314.
[22] E.V. Parkhomchuk, K.V. Fedotov, A.I. Lysikov, A.V. Polukhin, E.E. Vorobyeva, I. A. Shamanaeva, N.N. Sankova, D.O. Shestakova, D.M. Reshetnikov, A.V. Volf, A. V. Kleymenov, V.N. Parmon, Catalytic hydroprocessing of oil residues for marine fuel production, Fuel 341 (2023) 127714, https://doi.org/10.1016/j.fuel.2023.127714.
[23] Y. Zhang, T.R. Brown, G. Hu, R.C. Brown, Techno-economic analysis of two bio-oil upgrading pathways, Chem. Eng. J. 225 (2013) 895–904, https://doi.org/10.1016/j.cej.2013.01.030.
[24] E. Nejadmoghadam, O. Öhrman, D. Creaser, L. Olsson, Impact of dewatering on pyrolysis oil upgrading: A comparative study of properties and hydrodeoxygenation, Chem. Eng. J. 533 (2026) 174193, https://doi.org/10.1016/j.cej.2026.174193.
[25] V.L. Mangesh, S. Padmanabhan, S. Ganesan, D. PrabhudevRahul, T.Dinesh Kumar Reddy, Prospects of pyrolysis oil from plastic waste as fuel for diesel engines: A review, IOP Conf. Ser. Mater. Sci. Eng. 197 (2017) 012027, https://doi.org/10.1088/1757-899X/197/1/012027.
[26] F. Faisal, M.G. Rasul, M.I. Jahirul, Upgrading MSW pyrolysis oil through distillation and hydrotreatment for automobile engine applications: A short review, Energy Rep. 9 (2023) 555–560, https://doi.org/10.1016/j.egyr.2023.12.008.
[27] A. Sujithraj, P. Tamizhdurai, V.L. Mangesh, C. Kavitha, A. Subramani, P. Saravanan, P. Nisha, P. Sasikumar, Nadavala Siva Kumar, Salwa B. Alreshaidan, Ghzzai Almutairi, Ahmed S. Al-Fatesh, Renewable energy from waste plastic: Hydroprocessing of mixed waste plastic to diesel fuel utilizing Fe/Mo-Al_2O_3 catalyst, Process. Saf. Environ. Prot. 193 (2025) 683–695, https://doi.org/10.1016/j.psep.2024.11.028.
[28] M. Badlaoui, N.Y.P. Cao, W. Pejpichestakul, B. Celse, B. Guichard, M.T. Nguyen, N. Charon, J.W. Thybaut, Performance comparison of tire pyrolysis oils in hydrotreating toward high-quality fuel, Chem. Eng. J. 520 (2025) 165115, https://doi.org/10.1016/j.cej.2025.165115.
[29] S.H. Lim, H.H. Pham, E.H. Kwon, N.S. Nho, Optimizing the use of pyrolysis waste oil as a feedstock for the naphtha cracking process by hydrotreating and hydrocracking, Resour. Environ. Sustain. 22 (2025) 100277, https://doi.org/10.1016/j.resenv.2025.100277.
[30] Q. Hao, Z. Yang, B. Wu, J. Zhu, Z. Li, J. Liu, L. Ma, Study on the deactivation of Ni-based catalyst in the hydrotreating process of waste plastic pyrolysis oil, J. Anal. Appl. Pyrolysis 168 (2022) 105789, https://doi.org/10.1016/j.jaap.2022.105789.
[31] B.S. Yoon, C. Kim, G.J. Park, S.G. Jeon, C.H. Ko, Upgrading waste plastic pyrolysis oil via hydrotreating over sulfur-treated Ni-Mo/Al_2O_3 catalysts, Fuel 369 (2024) 131688, https://doi.org/10.1016/j.fuel.2024.131688.
[32] J. Seok, N.T.Y. Phan, J.C. Kim, H. Shin, M. Choi, Catalytic synergy between Lewis acidic alumina and Pt in hydrodechlorination for plastic chemical recycling, J. Am. Chem. Soc. 146 (2024) 23881–23890, https://doi.org/10.1021/jacs.4c06231.
[33] P. Straka, M. Auersvald, D. Vrtiška, H. Kittel, P. Šimáček, P. Vozka, Production of transportation fuels via hydrotreating of scrap tires pyrolysis oil, Chem. Eng. J. 460 (2023) 141764, https://doi.org/10.1016/j.cej.2023.141764.
[34] C. Ortega, M. Rezaei, V. Hessel, G. Kolb, Methanol to dimethyl ether conversion over a ZSM-5 catalyst: Intrinsic kinetic study on an external recycle reactor, Chem. Eng. J. 347 (2018) 741–753, https://doi.org/10.1016/j.cej.2018.04.160.
[35] A.S. Pushnov, Calculation of average bed porosity, Chem. Petrol. Eng. 42 (2006) 14–17, https://doi.org/10.1007/s10556-006-0045-x.
[36] Z. Guo, Z. Sun, N. Zhang, X. Cao, M. Ding, Mean porosity variations in packed bed of monosized spheres with small tube-to-particle diameter ratios, Powder Technol. 354 (2019) 842–853, https://doi.org/10.1016/j.powtec.2019.07.001.
[37] A.J. Otaru, A.R. Kennedy, Investigation of the Pressure Drop Across Packed Beds of Spherical Beads: Comparison of Empirical Models With Pore-Level Computational Fluid Dynamics Simulations, in: Journal of Fluids Engineering, 141, Transactions of the ASME, 2019, https://doi.org/10.1115/1.4042957.
[38] W. Zhang, K.E. Thompson, A.H. Reed, L. Beenken, Relationship between packing structure and porosity in fixed beds of equilateral cylindrical particles, Chem. Eng. Sci. 61 (2006) 8060–8074, https://doi.org/10.1016/j.ces.2006.09.036.
[39] M. Auersvald, M. Šiman, E.L. Vachková, J. Kroufek, P. Straka, G. Barzallo, P. Vozka, A comparative study of aromatic content in pyrolysis oils from waste plastics and tires: Assessing common refinery methods, Fuel 369 (2024) 131714, https://doi.org/10.1016/j.fuel.2024.131714.
[40] M. Auersvald, M. Šiman, P. Vozka, P. Straka, Quantitative determination of olefins in pyrolysis oils from waste plastics and tires using selective adsorption by Ag–SiO_2 followed by GC×GC-FID, Talanta 281 (2025) 126792, https://doi.org/10.1016/j.talanta.2024.126792.
[41] P. Straka, D. Maxa, M. Stas, A novel method for the separation of high-molecular-weight saturates from paraffinic petroleum based samples, Org. Geochem. 128 (2019) 63–70, https://doi.org/10.1016/j.orggeochem.2018.12.002.
[42] F. Campuzano, A.G.A. Jameel, W. Zhang, A.H. Emwas, A.F. Agudelo, J.D. Martínez, S.M. Sarathy, On the distillation of waste tire pyrolysis oil: A structural characterization of the derived fractions, Fuel 290 (2021) 120041, https://doi.org/10.1016/j.fuel.2020.120041.
[43] S. Wiriyaumpaiwong, J. Jamradloedluk, Distillation of pyrolytic oil obtained from fast pyrolysis of plastic wastes, Energy Proced. 138 (2017) 111–115, https://doi.org/10.1016/j.egypro.2017.10.071.
[44] S. Gulshan, H. Shafaghat, H. Yang, P. Evangelopoulos, W. Yang, Performance analysis and production of aromatics for ex situ catalytic pyrolysis of engineered WEEE, J. Anal. Appl. Pyrolysis 179 (2024) 106510, https://doi.org/10.1016/j.jaap.2024.106510.
[45] B.B. Perez-Martinez, A. Lopez-Urionabarrenechea, A. Serras-Malillos, E. Acha, B. M. Caballero, A. Asueta, S. Arnaiz, Influence of Feedstock Particle Size on the Certain Determination of Chlorine and Bromine in Pyrolysis Oils from Waste Electrical and Electronic Equipment Plastics, ACS Omega 9 (2024) 32593–32603, https://doi.org/10.1021/acsomega.4c01415.
[46] M. Wójcik-Bania, Clay minerals in Polysiloxane (silicone) systems, Polymer 313 (2024) 127743, https://doi.org/10.1016/j.polymer.2024.127743.
[47] Q. Yan, Y. Li, J. Zhao, Z. Yang, Z. Lei, Synthesis of a histidine-magnesium hydroxide curing agent and improving the flame retardant, smoke suppression of epoxy resin composites, Colloid Surf. A-Physicochem. Eng. Asp. 728 (2026) 138488, https://doi.org/10.1016/j.colsurfa.2025.138488.
[48] X. Li, X. Liu, Z. Lv, L. Dang, Construction of magnesium–molybdenum–phosphorus multi-component flame retardant and its performance in flexible PVC composites, RSC Adv. 15 (37) (2025) 30046–30061, https://doi.org/10.1039/d5ra04341g.
[49] Y. Li, Q. Su, Y. Leng, P. Sun, X. Han, M. Xu, X. Li, B. Li, Silane-modified magnesium oxide synergized with diphenyl chlorophosphate for high thermal conductivity and flame-retardant epoxy composites, Compos. Commun. 60 (2025) 102617, https://doi.org/10.1016/j.coco.2025.102617.

[50] W. Arjharn, P. Liplap, S. Maithomklang, K. Thammakul, S. Chuepeng, E. Sukjit, Distilled Waste Plastic Oil as Fuel for a Diesel Engine: Fuel Production, Combustion Characteristics, and Exhaust Gas Emissions, ACS Omega 7 (2022) 9720–9729, https://doi.org/10.1021/acsomega.1c07257.
[51] A.P. Silva, J.O. Bahú, R. Soccol, L. Rodríguez-Urrego, W.S. Fajardo-Moreno, H. Moya, J. León-Pulido, V.O. Cárdenas Concha, Naphtha Characterization (PIONA, Density, Distillation Curve and Sulfur Content): An Origin Comparison, Energies 16 (2023) 3568, https://doi.org/10.3390/en16083568.
[52] W. Zeb, T. De Somer, M. Roosen, P. Knockaert, M.Seifali Abbas-Abadi, U. Kresovic, J. Hogie, K.M. Van Geem, S. De Meester, Fractional distillation of waste plastic pyrolysis oil for isolating narrow hydrocarbons cuts, Fuel 379 (2025) 133055, https://doi.org/10.1016/j.fuel.2024.133055.
[53] L. Šindelářová, E.N. Luu, P. Vozka, Comparison of gas and kerosene oils chemical composition before and after hydrotreating using comprehensive two-dimensional gas chromatography, J. Chromatogr. Open. 2 (2022) 100068, https://doi.org/10.1016/j.jcoa.2022.100068.
[54] D. Ferdous, A.K. Dalai, J. Adjaye, Comparison of product selectivity during hydroprocessing of bitumen derived gas oil in the presence of $NiMo/Al_2O_3$ catalyst containing boron and phosphorus, Fuel 85 (9) (2006) 1286–1297, https://doi.org/10.1016/j.fuel.2005.11.018.
[55] M. Sajdak, A.J. Majewski, S. Sobek, G. Gałko, M. Ouadi, Design of experiments method into upgrading pyrolytic oil for sustainable aviation fuel additives by hydrotreating and hydrocracking, Waste Manag. 194 (2025) 258–269, https://doi.org/10.1016/j.wasman.2025.01.012.
[56] M.F. Wagenhofer, H. Shi, O.Y. Gutiérrez, A. Jentys, J.A. Lercher, Enhancing hydrogenation activity of Ni-Mo sulfide hydrodesulfurization catalysts, 2020. https://www.science.org.
[57] M.K. Prabhu, J.N. Louwen, E.T.C. Vogt, I.M.N. Groot, Hydrodesulfurization of methanethiol over Co-promoted MoS2 model catalysts, Nat. Commun. 15 (2024), https://doi.org/10.1038/s41467-024-51549-6.
[58] M.V. Bukhtiyarova, E.N. Vlasova, G.A. Bukhtiyarova, Hydroprocessing of biomass feedstock over sulfided CoMo-, NiMo-, and NiW-supported catalysts for bio-jet fuel component production: a review, Sustain. Energy Fuels 8 (2024) 3524–3544, https://doi.org/10.1039/d4se00302k.
[59] M. Auersvald, V. Krupka, D. Vrtiška, P. Šimáček, P. Straka, L. Kejla, 2023. Hydrotreating of waste plastic pyrolysis oil with increased chlorine and nitrogen content. PYROLIQ II - 2023: Pyrolysis and Liquefaction of Biomass and Wastes. Available at: https://dc.engconfintl.org/pyroliq_2023/13 (accessed on 14th May 2026).
[60] L. Lu, W. Li, Y. Cheng, M. Liu, Chemical recycling technologies for PVC waste and PVC-containing plastic waste: A review, Waste Manag. 166 (2023) 245–258, https://doi.org/10.1016/j.wasman.2023.05.012.
[61] J. Wang, Z. Xi, R. Gao, B. Niu, Z. Xu, Catalysis pyrolysis debromination from waste printed circuit boards: Catalysts selection, parameter effects, products, and mechanisms, Waste Manag. 191 (2025) 191–202, https://doi.org/10.1016/j.wasman.2024.11.009.
[62] L. Amodio, J. López, A. Souza, J. Cueto, H. Hernando, P. Pizarro, D. Serrano, Simultaneous removal of brominated and chlorinated species during the production of oils by e-waste plastics catalytic hydropyrolysis, J. Hazard. Mater. 465 (2024) 133357, https://doi.org/10.1016/j.jhazmat.2023.133357.
[63] L. Kaluža, D. Kubička, The comparison of Co, Ni, Mo, CoMo and NiMo sulfided catalysts in rapeseed oil hydrodeoxygenation, React. Kinet. Mech. Catal. 122 (2017) 333–341, https://doi.org/10.1007/s11144-017-1247-2.
[64] M.S. Kalem, Effect of fractional distillation pretreatment on fuel quality of plastic waste pyrolytic oils, Sep. Purif. Technol. 300 (2022) 121859, https://doi.org/10.1016/j.seppur.2022.121859.
[65] S. Hafeez, M. Van Haute, G. Manos, H.J. Karam, A. Constantinou, S.M. Al-Salem, Hydrotreatment over the Pt/Al_2O_3 Catalyst of Polyethylene-Derived Pyrolysis Oil and Wax, Energy Fuels 37 (2023) 16181–16185, https://doi.org/10.1021/acs.energyfuels.3c03152.
[66] E. Lazzari, M. Piparo, C. Mase, L. Levacher, P.H. Stefanuto, G. Purcaro, J.F. Focant, P. Giusti, Chemical elucidation of recycled plastic pyrolysis oils by means of GC×GC-PI-TOF-MS and GC-VUV, J. Anal. Appl. Pyrolysis 176 (2023) 106224, https://doi.org/10.1016/j.jaap.2023.106224.
[67] S. Cañete, S.D. González-Egido, L. Faba, S. Ordoñez, Efficient styrene removal from refuse-derived fuel pyrolysis oil using waste hydroprocessing catalysts, J. Anal. Appl. Pyrolysis 187 (2025) 106992, https://doi.org/10.1016/j.jaap.2025.106992.
[68] A.A. Gaile, G.D. Zalishchevskii, N.N. Gafur, L.V. Semenov, O.M. Varshavskii, N. P. Fedyanin, E.A. Kaifadzhyan, Separation of Aromatic Hydrocarbons from Reformate. Combined Extraction Fractionation–Extraction, Chem. Tech. Fuels Oils. 40 (2004) 131–136, https://doi.org/10.1023/B:CAFO.0000031891.84319.15.
[69] J. Wu, G. Chen, A. Chen, Z. Gao, X. Wu, H. Cheng, Y. Li, Y. Wang, Z. Qian, X. Zhang, C. Xu, Z. Chen, L. Zhang, Molecular-Level Modeling of Naphtha Continuous Catalytic Reforming Process, Chem. Eng. Sci. 309 (2025) 121430, https://doi.org/10.1016/j.ces.2025.121430.
[70] Q. Wang, B.J. Zhang, C. He, C.C. He, Q.L. Chen, Optimal design of a new aromatic extractive distillation process aided by a co-solvent mixture, Energy Proced. 105 (2017) 4927–4934, https://doi.org/10.1016/j.egypro.2017.03.984.
[71] V.L. Mangesh, P. Tamizhdurai, S. Umasankar, R. Palaniswamy, S. Narayanan, T. Augustine, R. Kumaran, Z.A. Alothman, M. Ouladsmane, M. Govindasamy, Hydroprocessing mixed waste plastics to obtain clean transport fuel, J. Clean. Prod. 358 (2022) 131952, https://doi.org/10.1016/j.jclepro.2022.131952.
[72] R. Vedavalli, P. Tamizhdurai, C. Kavitha, V.L. Mangesh, G.S.V.Seshu Kumar, P. Saravanan, A. Subramani, P. Sasikumar, N.S. Kumar, S.B. Alreshaidan, A. I. Alromaeh, A.S. Al-Fatesh, Catalytic conversion of plastic waste into diesel fuel through pyrolysis and hydroprocessing, Process. Saf. Environ. Prot. 193 (2025) 327–339, https://doi.org/10.1016/j.psep.2024.11.029.
[73] R. Prajapati, E.O. Zaborowski, H. Lu, N. Rajagopalan, B.K. Sharma, B.R. Moser, N. Kumar, Production of a Sustainable Aviation Fuel Additive from Waste Polystyrene, ACS Sustain. Chem. Eng. 13 (1) (2025) 212–219, https://doi.org/10.1021/acssuschemeng.4c06748.
[74] N.A. Romanova, V.S. Leont'ev, A.S. Khrekin, Production of Commercial Naphthalene by Coal-Tar Processing, Coke Chem. 61 (2018) 453–456, https://doi.org/10.3103/S1068364X18110078.
[75] H. de Paz Carmona, J. Horáček, A. Brito Alayón, J.J. Macías Hernández, Suitability of used frying oil for co-processing with atmospheric gas oil, Fuel 214 (2018) 165–173, https://doi.org/10.1016/j.fuel.2017.10.133.
[76] H. de Paz Carmona, J. Kocík, J.M. Hidalgo Herrador, A. Vráblík, Effectiveness of Mo, NiMo, and CoMo catalysts for co-hydroprocessing furfural-acetone aldol condensation adducts with atmospheric gas oil to produce biofuels, Fuel 355 (2024) 129489, https://doi.org/10.1016/j.fuel.2023.129489.
[77] A. Dimitriadis, G. Meletidis, U. Pfisterer, M. Auersvald, D. Kubička, S. Bezergianni, Integration of stabilized bio-oil in light cycle oil hydrotreatment unit targeting hybrid fuels, Fuel Process. Technol. 230 (2022) 107220, https://doi.org/10.1016/j.fuproc.2022.107220.
[78] R. Palos, A. Gutiérrez, F.J. Vela, M. Olazar, J.M. Arandes, J. Bilbao, Waste Refinery: The Valorization of Waste Plastics and End-of-Life Tires in Refinery Units. A Review, Energy Fuels 35 (2021) 3529–3557, https://doi.org/10.1021/acs.energyfuels.0c03918?ref=pdf.
[79] D. Schlehöfer, H. Kittel, A. Vráblík, M. Dragoun, Compatibility of feed for hydrocracking and FCC with scrap tires and waste plastics pyrolysis oil residue, J. Energy Inst. 123 (2025) 102283. https://doi.org/10.1016/j.joei.2025.102283.